國立臺灣大學生命科學院基因體與系統生物學位學程

碩士論文

Genome and Systems Biology Degree Program

College of Life Science

National Taiwan University

Master's Thesis

臺灣殼斗科森林之真菌菌相探討

Mycobiome of Taiwanese Fagaceae Forests

林婕蘋

Chieh-Ping Lin

指導教授：蔡怡陞 博士

Advisor: Isheng Jason Tsai, Ph.D.

中華民國 113 年 1 月

January 2024

doi:10.6342/NTU202304440

國立臺灣大學碩士學位論文
口試委員會審定書

MASTER THESIS ACCEPTANCE CERTIFICATE
NATIONAL TAIWAN UNIVERSITY

台灣殼斗科森林之真菌菌相探討

Mycobiome of Taiwanese Fagaceae Forests

本論文係林婕蘋（R10B48002）在國立臺灣大學基因體與系統生物學位學程完成之碩士學位論文，於民國 113 年 1 月 16 日承下列考試委員審查通過及口試及格，特此證明。

The undersigned, appointed by the Genome and Systems Biology Degree Program on 16th, January, 2024 have examined a master thesis entitled above presented by Chieh-Ping Lin (R10B48002) candidate and hereby certify that it is worthy of acceptance.

口試委員 Oral examination committee:

（指導教授 Advisor）

系（所、學位學程）主管 Director:

ACKNOWLEDGEMENT/致謝

研究所的旅程像是場回合制 RPG，要學著在有限的回合中囤積糧草與資源打魔王，同時要面對使人焦頭爛額的隨機事件與臨時任務，過程中，會遇到讓人崩潰的遊戲惡意，會遇到在團戰毫無貢獻的無用隊友，但也同時會遇到各式讓人萬幸、珍惜的人事物，縱使過程不盡完美，但回憶起也都是有趣的。

大學四年，跟著真菌室一邊趕著評鑑一邊讀著期中期末，另一手還不忘參與系上各式活動的籌備，寒暑假也積極參與實習，感謝帶我成長的啟予老師、國維、玠皜學長，感謝當年鼓勵我踏出那一步的許惇偉老師，也感謝在推甄時勇於轉換跑道的我。

碩班的生活既充實又有趣，有在上課時每每讓我無比佩服的優秀同學，有總能讓我放心做自己的實驗室，以及使口委都不可置信的龐大樣本數。這兩年半間，除了碩士論文的森林真菌相之外，還做了水樣 eDNA、海洋生物的 mitogenome，還在延畢期間去南美洲待了兩個月，踏上了馬丘比丘、彩虹山、玻利維亞天空之境、並且在智利釀了一個月的酒，參與的計畫多元到每每使我難以與家人解釋近況，而一切的一切都要感謝總是相信我的能力，並讓我去做各式嘗試的指導教授 Jason，身為一個自由的靈魂，很榮幸且幸運可以找到合適的容身之處。

Jason 是個重視學生想法與發展的盡責指導教授，也是少數還會親身參與實驗(分析)的教授，在眾多要務與會議纏身的前提下，仍堅持使每周兩小時以上的進度報告成為日常，老師直接、明瞭且開放討論的風格，對每個結果細細雕琢的精神， 讓每次的會議過後都能有新的啟發與方向，也充分展示了老師對研究的熱情與謹慎；Jason 也是個有耐心、具同理心的不可多得的優秀導師，

doi:10.6342/NTU202304440

深深感謝他在我被失敗及挫折感壟罩時，及時發現並接住了我。兩年半來，不論是人員更替的時候，每次採樣回來的兩個月都處理樣本到半夜的時候，還是實驗屢屢碰壁，覺得很辛苦、憂鬱的時候，我都從未後悔加入實驗室的決定，因為我在這裡獲得的改變跟成長是超乎預期的，感謝 Jason 提供的資源、在背後的支持，以及一直以來的鼓勵。實驗室的主題跨足了線蟲、真菌、植物、海洋生物等多個領域，看似毫無關聯，但每次談起各項研究進展時，老師那閃著光芒的眼神，總能說明好奇心便是串連起一切的原因，以身作則示範了科學始於好奇，終於實踐，深感佩服。

感謝在實驗及分析上領我入門的 Tom 大大，感謝帶我去採樣，並替大家扛下眾多行政作業的育菁，以及曾經參與採樣的蕭禎、Daphne、佳啟、維廷，感謝在分析上與系上事務總會對我伸出援手的 Rubie，感謝在組 mitogenome 上提供各式幫助，並在寫論文及準備口試的過程中，不吝提供意見的宜謙；心理素質強大，對小毛氈苔執著到應該要寫進教科書的培峰，出國前每個晚上留下來和我小酌看動畫的法喜大師蕭禎，雖然找到教職，仍是實驗室強大後盾的實驗神手阿棉。這是一個組織極扁平化的實驗室，沒有令人卻步的階級關係，也沒有消耗心神的人際關係，只有啤酒、不斷擴張的零食庫與令人稱羨的師徒關係，感謝大家成為我碩士生活的養分。

最後，感謝總是承攬我各式情緒，聽我分享荒謬事跡、壓力大時陪我打遊戲的好友們；與即使不理解，也總是尊重我的各項決定的家人；還有教我正視情緒，總是理性分析，並帶領我走出黑暗的諮商師艾恩。

也感謝無數次想放棄，但始終撐下來的我自己。

end(masterdegree)

doi:10.6342/NTU202304440

中文摘要

真菌在自然環境中扮演著多樣且重要的角色，其豐富性可直接反映生態系統的穩定性和功能性，故對於永續生態管理，了解森林真菌群是至關重要的。本研究中，我們以八種殼斗科物種作為研究材料，採集樹葉、枝條、落葉及土壤等四種介質，共 864 個樣本的真菌 ITS2 區域進行擴增，再以高通量分子條碼(metabarcoding) 技術，調查臺灣熱帶及亞熱帶森林的真菌多樣性及組成。採集點之海拔落於 500 至 2500 公尺之間。分析結果共鑑定了 11,600 個擴增子序列變異(Amplicon sequencing variants; ASVs)，平均每樣本有 69 個，於其中有兩個普遍存在且無顯著生態為偏好的 ASV，分類上分別屬於 *Cladosporium* sp. 及 *Pyrenochaetopsis* sp.。由樹葉、枝條及落葉組成的葉際中，共享的 ASV 有 12 個，平均佔樣本相對豐度的 5%。在 α 多樣性分析上，落葉的真菌多樣性最高，其次為葉子及枝條，而土壤在這四種介質中則最低。在真菌的組成上，受地理位置影響最為顯著，其次為介質、季節及寄主物種。高海拔的樣本(超過 1500 公尺)在真菌組成上較低海拔樣本(低於 800 公尺)更為相似。分析結果顯示，同物種寄主的真菌組成在不同森林中存在差異，其相似度會隨著海拔高度的增加而升高。季節變化對真菌整體多樣性有顯著影響，其中長期的降雨量為主導因素。在組成比例上，子囊菌門的真菌佔比最高，又以一 *Cladosporium* sp.最為優勢。這佔有高豐度的 *Cladosporium* ASV 也是本研究分析結果中唯一的關鍵物種，且後續藉由長片段擴增子定序技術(Long amplicon sequencing)驗證為單一物種。我們的研究深入了解了臺灣闊葉林的真菌多樣性，揭示了海拔驅動的變化、季節影響，以及關鍵物種— *Clasoporium* sp.的優勢。

關鍵字：高通量分子條碼、森林真菌菌相、殼斗科、熱帶及亞熱帶森林

doi:10.6342/NTU202304440

ABSTRACT

Diversity of the fungal community directly reflects the stability of the whole ecological system. Understanding the forest mycobiome is crucial for managing ecosystems sustainably. In this study, we investigated the fungal diversity of seven Fagaceae species in tropical and subtropical forests in Taiwan using a metabarcoding approach by sequencing ITS3/ITS4 amplicon in a total of 864 samples across four different substrates (leaf, twig, litter and soil). The locations of the trees range in altitude from 500 to 2500 meters. We identified a total of 11,600 amplicon sequencing variants (ASVs) with averaging 69 ASVs per sample. There were two ubiquitous ASVs, *Cladosporium* and *Pyrenochaetopsis*, with unclassified species and no significant niche preference. Phyllosphere, including leaf, twig, and litter, shared 12 ASVs, accounting on average 5% of samples' relative abundance. Across substrates, higher α-diversity was observed in litter than twig and leaf, while soil had the lowest diversity. Mycobiome composition was most significantly influenced by host tree's location, followed by substrates, season, and host species. Samples from high altitudes (over 1500 m) had a similar composition compared to those from low altitudes (below 800 m). Our results revealed that the mycobiome composition varies across forests from same host species, and had a tendency of being similar along with the altitude. Seasonal changes have a significant influence on the total fungal diversity, with long-term precipitation serves as the predominant factor. The majority of the observed mycobiome was composed of Ascomycota taxa, with a *Cladosporium* sp. as the dominant ASV. The prevalent *Cladosporium* ASV is also detected as the only keystone species in our study and is verified as a single species via long amplicon sequencing of the full ribosomal operon. Our study brings insight into the fungal diversity of Taiwanese broadleaf forests,

doi:10.6342/NTU202304440

revealing altitude-driven variations, seasonal influences, and the dominance of the keystone species — *Cladosporium* sp.

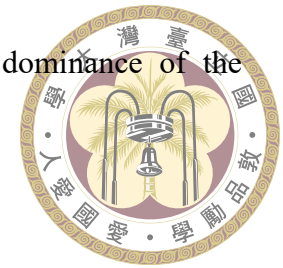

Keywords: Metabarcoding, Mycobiome, Epiphytic fungi, Fagaceae, Tropical and subtropical forests.

doi:10.6342/NTU202304440

CONTENTS

口試委員審定書 i

ACKNOWLEDGEMENT/致謝 ii

中文摘要 iv

ABSTRACT v

CONTENTS vii

LIST OF FIGURES viii

LIST OF SUPPLEMENTARY MATERIALS ix

CHAPTER 1. Introduction 1

CHAPTER 2. Materials and Methods 5

2.1 Sample collection, preprocessing and DNA extraction 5

2.2 Sample preprocessing and DNA extraction 6

2.3 Amplicon library construction and sequencing 7

2.4 Statistical analyses 8

2.5 Network analysis 9

2.6 Long amplicon sequencing 9

CHAPTER 3. Results 12

3.1 Fungal diversity and composition differences through time among forests with the same host species and niches 12

3.2 Biological replicate consistency of the forest mycobiome 18

3.3 Effects of abiotic factor on forest mycobiome 19

3.4 Co-occurrence network analysis and putative keystone species 21

3.5 Finding the exact ASV of putative keystone species by long amplicon sequencing 24

CHAPTER 4. Discussions 26

References 29

Supplementary Materials 39

doi:10.6342/NTU202304440

LIST OF FIGURES

FIG. 1. Map of survey sites. 6

FIG. 2. Fungal relative abundance composition and dominant species. 13

FIG. 3. Box plot of mycobiome α-diversity across substrates and host species. 15

FIG. 4. Mycobiota composition differences among seasons, substrates, host species, and locations. 16

FIG. 5. Number and relative abundance of endemic and ubiquitous ASVs among compartments. 17

FIG. 6. The biological replicates consistency among batches and compartments. 19

FIG. 7. Variations in mycobiome composition differences due to precipitation. 20

FIG. 8. Co-occurrence networks with significant strong correlations between ASVs across seasons and substrates. 23

FIG. 9. Relative abundance of *Cladosporium* in long amplicon data. 25

FIG. 10. Percent identity of *Cladosporium* sp. strain KR14 and ASVs from long amplicon sequencin. 25

doi:10.6342/NTU202304440

LIST OF SUPPLEMENTARY MATERIALS

FIG. S1. Bar plot of mean of guild relative abundance of unique and shared ASVs of the intersections among four compartments. 39

FIG. S2. Relative abundance of ubiquitous ASVs among compartments. 39

FIG. S3. Co-occurrence networks illustrating robust correlations among ASVs across seasons and substrates. 40

FIG. S4. The proportion changes of functional guild nodes in different seasons. 41

FIG. S5. The connectively within and among modules of vertices in the co-occurrence network. 42

Table S1. Tree information 43

Table S2. Survey sites weather information 45

doi:10.6342/NTU202304440

CHAPTER 1.

Introduction

As fungi play numerous crucial roles in the environment, fungal diversity directly reflects the stability and functioning of the ecosystem (Liu et al., 2022; Wagg et al., 2019). Fungi as decomposers in the carbon cycle are essential for organic matter decomposition and nutrient cycling, which transforms the materials from unavailable to absorbable for plants. Also, several studies have demonstrated that the interactions between some fungi and their plant hosts beneficially affect plant development, survival, nutrient uptake, fitness, health, and ecosystem functions (Bai et al., 2018; Rosier et al., 2016; Sasse et al., 2018; Yan et al., 2019). Fungi are intricately involved in nearly every stage of plant growth, from germination to seedling developing, blooming, decline and to decomposition of plant material (Peay et al., 2016). Their diverse roles, from mutualistic partnerships to pathogenic interactions and decomposition, highlight the importance of understanding fungal composition for maintaining ecosystem health and plant vitality. Hence, understanding the fungi diversity and their interaction with the plant is a crucial step for managing ecosystems sustainably, which could serve as a potential criterion for assessing the health status of forests in the future (Baldrian et al., 2023).

Next-generation sequencing (NGS) gives us a new perspective on ecological studies. As sequence-based species delimitation approaches gain traction, DNA metabarcoding has grown in importance in fungal diversity research. (Meiser et al., 2014). The efficient and high-throughput approach provides insights into the presence and diversity of species without direct observation and allows us to assess the whole communities from a single sample. Additionally, it overcomes the constraint of traditional methods, which struggle to detect unculturable and low-abundance species. However, due to the sequence length

doi:10.6342/NTU202304440

limitation of NGS, including 454 pyrosequencing and Illumina sequencing, it is necessary to amplify and analyze the ITS1 or ITS2 separately. It faced another issue that the researchers in fungal taxonomy and systematics have observed that the interspecific ITS divergence between sister species varies significantly and that, in certain cases, closely related species may have identical ITS sequences (Blaalid et al., 2013; Garnica et al., 2016; Hoang et al., 2019). That is, even the full length of ITS is not enough for identifying certain species. The improvement of read length in third-generation sequencing solves this problem. By sequencing more complete fungal ribosomal operons, more comprehensive genetic information can be provided to refine taxonomic assignment (Kauserud, 2023).

Current mycobiome studies mostly focus on terrestrial ecosystems compared to animal and aquatic ecosystems. In comparison to research into other parts of the plant, there is still a significant bias against soil, especially in the rhizosphere (Peay et al., 2016). Furthermore, whereas tropical and subtropical forests make up about 56% of the global forest area and harbor 42.8% of all trees worldwide, most studies in forest microbiomes have focused on temperate and boreal forests (Baldrian, 2017; Ehrenberg, 2015). Tropical and subtropical forests are the most diverse forest. These forests exhibit high levels of primary productivity due to warm and humid conditions, resulting in lush vegetation, making it critical for biodiversity conservation, carbon sequestration and climate regulation (Koch & Kaplan, 2022).

The aboveground plant surface, so called phyllosphere, is a unique and challenging habitat for microbial colonisation which is constrained by water, nutrients, and exposure to intense UV radiation (Stone et al., 2018). Environmental factors, including temperature, raining, solar radiation, and wind, play pivotal roles in shaping the composition and size

doi:10.6342/NTU202304440

of microbial communities in phyllosphere (Aydogan et al., 2018; Leveau, 2019; Schiro et al., 2018; Truchado et al., 2019). While fungal phytopathogens are the primary cause of plant diseases, certain fungi also have the ability to defend their hosts against plant pathogens; and therefore, compositional differences between functional guilds can affect host fitness (Łaźniewska et al., 2012; Syed Ab Rahman et al., 2018). Moreover, the composition of fungi in the forest can change seasonally or over time due to various factors, such as biotic/abiotic disturbance or climate change. Faced on the environmental disturbances such as climate change and habitat loss, it is essential to monitor and investigate the response of mycobiome during different climates. Therefore, to ensure the sustainable management of the forest environment, it is necessary to gain a deeper understanding of the complexity of fungi diversity in different forest ecosystems (Tomao et al., 2020).

Forested lands cover 60.7% of Taiwanese territory, which is twice more than the global average of 30.2%, forming the largest ecosystem in Taiwan (Lin et al., 2021). According to the Taiwan Forest and Nature Conservation Agency investigation in 2020, natural forests account for 85.6% of the total forest area, 62.6% of which are broadleaf forests, while the remaining portion is composed of coniferous (24%) and mixed forests (13.4%) (https://www.forest.gov.tw). Taiwanese forests own various vegetation types, with broad-leaved forests being dominated by Fagaceae, Araliaceae, Lauraceae, Magnoliaceae and Theaceae (Li et al., 2013).

Our research is a large-scale investigation of the tropical and subtropical forest mycobiota in Taiwan. In this study, we investigated the mycobiome diversity of seven Fagaceae species in three tropical and subtropical Taiwanese forests at two different time points. Using the metabarcoding approach by ITS3/ITS4 amplicon-targeted Illumina

doi:10.6342/NTU202304440

Miseq sequencing in a total of 864 samples across four different substrates (leaf, twig, litter and topsoil). The survey sites of the trees range in altitude from 500 to 2500 meters. This study aims to i) investigate the differences in fungal diversity among forests with the same host species and niches; ii) understand the mycobiome composition changes during time; iii) examine the replicates consistency across substrates, hosts and environments; iv) use the co-occurrence network analysis to explore the keystone species of the entire forest; v) and finally, utilize Nanopore long amplicon sequencing to delimit the composition of the keystone ASV.

doi:10.6342/NTU202304440

CHAPTER 2.

Materials and Methods

2.1 Sample collection

To compare the mycobiome changes and differences during the time and between locations, we collected leaf, twig, litter and soil samples of 38 trees from seven Fagaceae species (*Quercus stenophylloides* n=14, *Quercus glauca* n=7, *Quercus morii* n=2, *Quercus pachyloma* n=3, *Castanopsis fargesii* n=2, *Lithocarpus hancei* n=5, *Lithocarpus glaber* n=5) from Puli Township and Ren'ai Township, Nantou County and Fushan Botanical Garden, Yilan County in Taiwan (Fig. 1) at two time points. The samples we obtained at Fushan Botanical Garden were from artificial Fagaceae woodlands. Samples from Nantou were harvested on April 18th-19th, 2022 and October 24th -26th, 2022. Samples from Fushan Botanical Garden were collected on July 1st, 2022 and December 26th, 2022. For collection, we originally chose 18 trees per survey site (a total of 36); however, after we discovered two of them decayed at the second time point (SPA0446 and SPA0457), we chose two more trees (SP0472 and SPA0487) instead. We sampled a total of 864 samples across four substrates and three replicates for each sample (216 samples for each substrate). After collection, samples were kept refrigerated at 4℃ after collection until sample preparation was completed.

doi:10.6342/NTU202304440

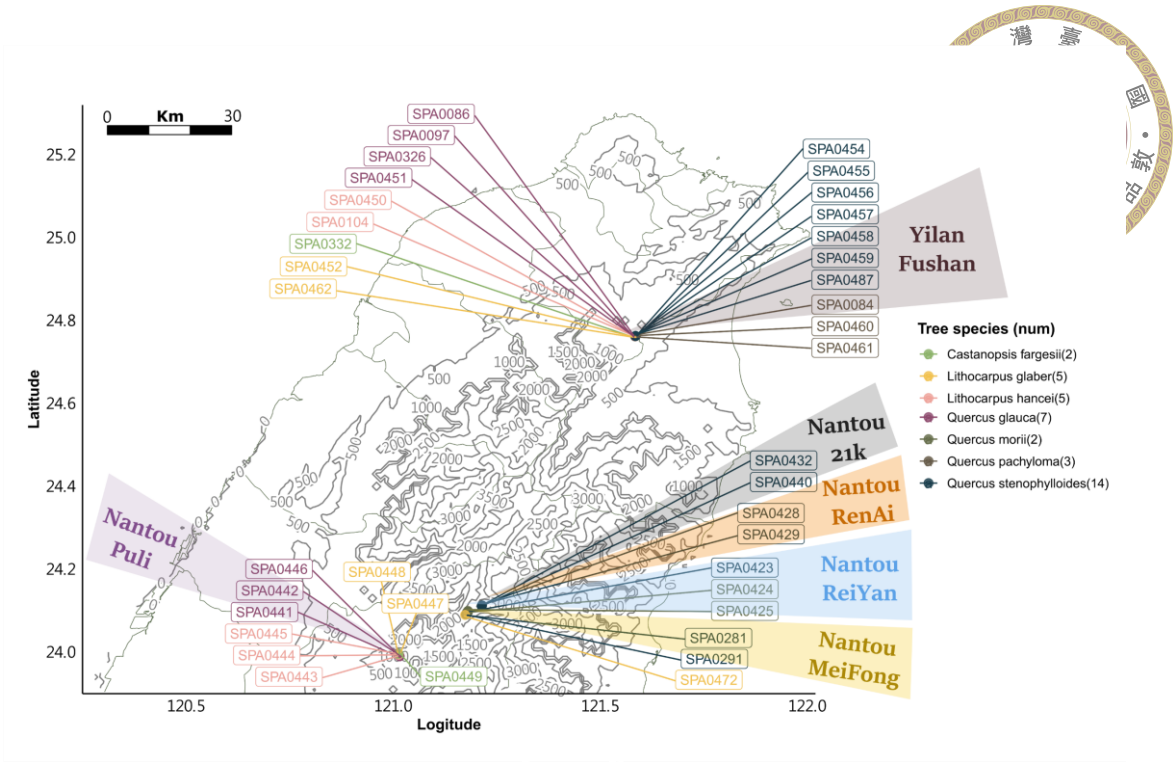

Figure 1. Map of survey sites. Tree-specific GPS data were complemented in Table S1.

2.2 Sample preprocessing and DNA extraction

The amount of leaf and litter in a sample range from 15 to 45. For sample leaf, twig and litter, the sample preprocessing procedures are as detailed in our previous study (Lee et al., 2022). After a series of sample preparation steps, eDNA on the surface of samples was collected on the 0.22 μm PES membrane of the filtration cup (Jet Bio-Filtration Co., Cat. FPE214250). To assess the background noise in the preprocessing step, three sterilized filter papers with no field samples were processed as the description above. The total nucleic acid was then extracted using the DNeasy PowerWater kit (QIAGEN; Cat. 14900-50-NF) following the manufacturer's instructions.

The topsoil samples were collected around the tree from a distance of 10 cm to 1 m, depending on how near we can reach the tree. The topsoil samples were first sieved using 2 mm steel mesh to remove plant debris, insects and rocks. Total nucleic acid was extracted from approximately 0.25 g of soil using the DNeasy PowerSoil Pro kit

doi:10.6342/NTU202304440

(QIANGEN, Cat. 47014) as instructed by the manufacturer. Precellys 24 Touch (Bertin Technologies, Cat. P002391-P24T0-A.0) was employed in the homogenization step. The homogenizer cycle was 5000 rpm for 90 sec, pause for 15 sec, and 5000 rpm for 90 sec. The extracted DNA was quantitated with Invitrogen Qubit 4 fluorometer (Invitrogen) and NanoDrop 1000 (ThermoFisher) and were stored at -20℃ until the amplicon library proceeded.

2.3 Amplicon library construction and sequencing

Amplicon libraries were constructed as previously described (Tedersoo et al., 2014) using forward primer ITS3ngs (5-CANCGATGAAGAACGYRG-3') and reverse primer ITS4ngsUni (5'-CCTSCSCTTANTDATATGC-3') (Tedersoo et al., 2015; Tedersoo & Lindahl, 2016) to amplify the ITS2 region. The PCR cocktail contained 50 ng of DNA extract, 2 µl of each 10 µM primer, 8 µl 5x HOT FIREPol Blend Master Mix (Solis Biodyne, Cat. 04-27-00115), 1 µl of 25 mM $MgCl_2$ and ddH_20 to 40 µl. We used extracted DNA of *Saccharomyces kudriavzevii*, *S. paradoxus* and *S. cerevisiae* as positive control to determine the false positive rate in the sequencing data. The thermal cycling conditions consisted of an initial denaturation at 95℃ for 12 min, followed by 35 cycles of denaturation at 95℃ for 20 sec, annealing at 55℃ for 30 sec, and extension at 72℃ for 1 min, finishing with a final cycle at 72℃ for 7 min. Amplicons were normalized to equal DNA quantity (approximately 25 ng) using SequalPrep^{TM} Normalization Plate Kit (Invitrogen, ID: A1051001) according to the manufacturer's instructions before pooling. The pooled library was concentrated to 10 ng/µl using AMPure XP (Beckman Coulter, ID: A63881). Each batch produced two plates of the library. Libraries were sequenced by Illumina Miseq PE300 sequencing platform with equal molar pooling and 20% Phix.

doi:10.6342/NTU202304440

2.4 Statistical analyses

The raw sequencing data was imported and demultiplexed using *sabre* (v1.0; https://github.com/najoshi/sabre) with a 1 bp mismatch allowed. Sequencing quality was examined using *FastQC* (v0.11.9; https://github.com/s-andrews/FastQC). The reads without attached primer sequences were discarded with *usearch* (v11.0.667; Edgar, 2016). The forward and reverse primer sequences were trimmed using *Cutadapt* (v4.4; Martin, 2011). The filtered and trimmed sequences were proceeded following *Qiime2* (v2023.5.1; Bolyen et al., 2019) pipeline to filter reads with a quality threshold of Qscore > 20 and to denoise into amplicon sequence variants (ASVs). The ASV's taxonomy was assigned using *constax* (v2.0.18; Liber et al., 2021) with UNITE Fungal database (v9.0; Abarenkov et al., 2010). And annotated the fungal guild using *FUNGuild* (v1.2; Nguyen et al., 2016).

Data processing and analyzing as following were performed in the R-studio environment (v2023.06; RStudio Team, 2020). And the taxonomy levels were updated using R's package *rgbif* (v3.7.7; Chamberlain & Boettiger, 2017). The background reads in the data were subtracted according to the median read number in the negative controls. In order to minimize the false positive ASVs in the dataset, the ASVs were filtered with a relative abundance of less than 0.1 % in each sample based on the results of positive controls. Preprocessed sequencing data were analyzed with *phyloseq* (v1.40.0; McMurdie & Holmes, 2013). Analyses based on merged data were produced by first rarefying the sample triplicates to the lowest read number (minimum: 5,000) and then merged by adding all of the sample reads. Figures were generated using *ggplot2* (v3.4.2; Villanueva & Chen, 2019). The sampling locations were annotated the sampling locations using *ggspatial* (v1.1.9; https://CRAN.R-project.org/package=ggspatial), *metR* (v0.14.0; https://github.com/eliocamp/metR) and *ggrepel* (v0.9.3; https://CRAN.R-project.org/package=ggrepel). Statistical significance test of the alpha diversity index was

doi:10.6342/NTU202304440

performed using HSD.test function in *agricole* package (v1.3.7; https://github.com/myaseen208/agricolae). The *UpSetR* package was performed to visualize the endemic and ubiquitous ASVs through the environments, with ASVs filtering by appearing in more than 25% of the environments (v1.4.0; https://CRAN.R-project.org/package=UpSetR).

2.5 Network analysis

Merged data of leaf, twig and litter were first rarefied to 15,000 reads per sample while soil data were rarefied to 10,000 reads per sample. Afterward, we employed a 50% threshold to filter the ASVs of the rarefied data based on their prevalence. This meant that an ASV could only be retained if it was present in more than 50% of the substrate. The correlation index was calculated using *FastSpar* (v1.0.0; Friedman & Alm, 2012; Watts et al., 2019Friedman & Alm, 2012; Watts et al., 2019) with 100 iteration. And we filtered the correlation data by their significance (false positive adjusted p-value $\leqq$ 0.05) and strong correlation (SparCC $\geqq$ 0.6 or SparCC $\leqq$ -0.6). The co-occurrence networks were visualized using *igraph* (Csardi & Nepusz, 2006). To find the putative keystone taxa, we estimated the Zi and Pi values of each node in the co-occurrence by the function within_module_deg_z_score and part_coeff of R package *brainGraph* (v3.0.0; https://CRAN.R-project.org/package=brainGraph).

2.6 Long amplicon sequencing

Long amplicon library preparation was referred to D'Andreano et al., 2021, using forward primer SR1R-Fw (5'- TTTCTGTTGGTGCTGATATTGCTACCTGGTTGATY CTGCCAGT) and reverse primer LR12-R (5'-ACTTGCCTGTCGCTCTATCTTGACT

doi:10.6342/NTU202304440

TAGAGGCGTTCAG-3') (Vilgalys lab, 1992) with optimized annealing temperature in the PCR program. The PCR reaction mixture consisted of 50 ng of DNA extract, 2 µl each of 10 µM forward and reverse primers, 20 µl of 2x KAPA HiFi HotStart ReadyMix (KAPA Biosystems, ID. KK2601), 1 µl of 25 mM $MgCl_2$, and ddH_2O adjusted to a total volume of 40 µl. The thermal cycling program initiated with a denaturation step at 95℃ for 3 min, followed by 25 cycles of denaturation at 98℃ for 20 sec, annealing at 58℃ for 30 sec, and extension at 72℃ for 6 min. The profile concluded with a final extension step at 72℃ for 10 min. The amplicons were purified using AMPure XP (Beckman Coulter, ID: A63881) and then ligated to the sample index using the Ligation sequencing amplicons-native barcoding kit 24 V14 (Oxford Nanopore Technologies, ID. SQK-NBD114.24) following the manufacturer instructions. The library was pooled with equal molar of barcoded amplicons (120 ng in total). The sequencing was performed on GidION using flow cell R10.4.1 (FLO-MIN114; flow cell number: FAW86351) for two runs. The second run was first washed by EXP-WSH004 and the same amount of library was loaded and sequenced again. The base-calling and demultiplexing step was conducted using dorado (v0.4.1; https://github.com/nanoporetech/dorado) in duplex mode.

The sequencing adaptors of raw reads were trimmed using *Porechop* (v0.2.4; https://github.com/rrwick/Porechop) with the parameter of adapter threshold set to 100 and the minimum split read size set to 2,000. The primer sequences were trimmed using *Cutadapt* (v4.5; Martin, 2011) with the maximum allowed error rate of 0.2 and a length filter of 2,500 to 6,500. Reads without containing both primers were discarded to exclude incompletely amplified or sequenced reads. *fastp* (0.23.4; Chen et al., 2018) was used to filter reads according to an average quality of 20. Based on the results of the positive control, in which the genome has been sequenced previously, the demultiplexed and trimmed sequencing data were processed with *usearch* (v11.0.667; Edgar, 2013). The

doi:10.6342/NTU202304440

filtered reads were then dereplicated into unique sequences and singletons were removed. Filtered unique sequences were denoised into amplicon sequencing variants (ASVs) using the *unoise3* algorithm (Edgar, 2016) and tabulated using the *otutab* function with an identity of 99%. The ASV's taxonomy was assigned using *blastn* (v2.14.0; Camacho et al., 2009) against the NCBI database (Sayers et al., 2022). The ASV's sequence integrity was detected using ITSx (v1.1.3; Bengtsson-Palme et al., 2013), and sequences without complete region annotation were discarded to exclude chimera.

doi:10.6342/NTU202304440

CHAPTER 3.

Results

3.1 Fungal diversity and composition differences through time among forests with the same host species and niches

By amplifying and sequencing the ITS2 region of fungi, we quantified the relative abundances of mycobiome amongst four compartments (leaf, twig, litter, and soil) and two seasons. After quality filtering and primer trimming to the raw data, 46,317,215 paired reads were obtained from 49,814,471 paired reads. We acquired 19,002,154 sequences after denoising, merging, and false positive ASV removing, which were then identified into 11,600 amplicon sequencing variants (ASVs) with an average of 69 ASVs per sample.

The ASVs were classified into seven phyla with 14.4% remaining unclassified. The overall fungal communities were dominated by Ascomycota (55.62%), followed by Basidiomycota (26.6%), Zygomycota (10.46%), Glomeromycota (0.40%), Chytridiomycota (0.39%), and Blastocladiomycota (0.02%) (Fig. 2a). We found that ASV1, an unidentified *Cladosporium*, was the most dominant ASV which is present in 332/736 samples with an average relative abundance of 2.28% (Fig. 2b). This ASV was especially prevalent in litter and leaf and have an average relative abundance of 3.51% and 2.98%, respectively, compared to 0.005% in other ASVs.

doi:10.6342/NTU202304440

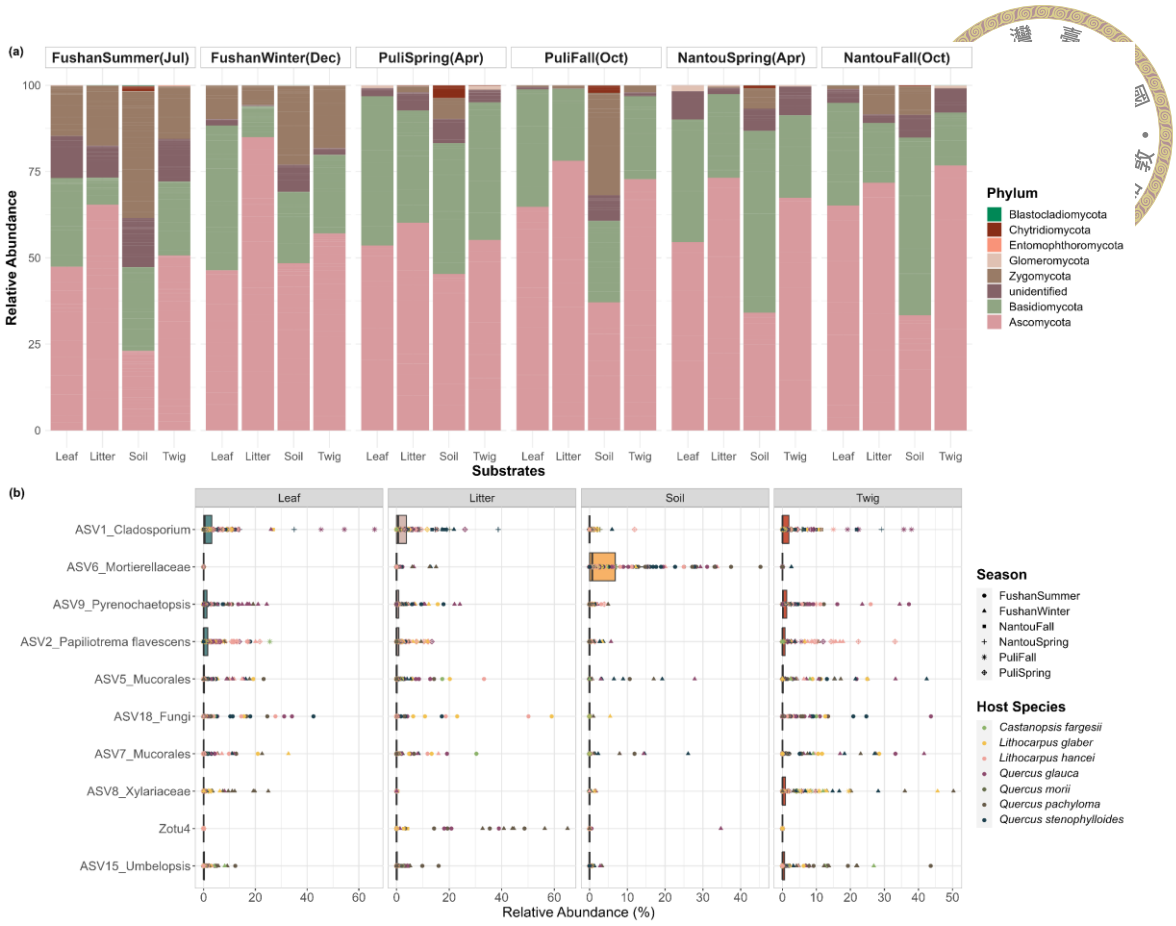

Figure 2. Fungal relative abundance composition and dominant species. (a) Bar plot of fungal phyla relative abundance across batches; (b) Boxplot of Top 10 ASVs' relative abundance across samples. Each dot represents one sample, the color indicates the host species and the shape denotes the collection seasons.

The α-diversity was calculated using Chao1 index and Shannon's diversity index to estimate the ASV richness and evenness of the fungal communities across substrates, host species, and seasons. The overall mycobiome α-diversity varied among substrates. In the total microbiota, higher α-diversity, including ASV richness and evenness, was observed in litter (73 ± 27 ASVs on average) than in twig (65 ± 23 ASVs on average) and leaf (63 ± 21 ASVs on average), while soil (58 ± 22 ASVs on average) had the lowest

doi:10.6342/NTU202304440

diversity. Season serves as another significant driver of the fungal communities (PERMANOVA $F_{5,663}$ = 2342.9430, R^2 = 0.80, $p < 0.001$). Yilan Fushan's mycobiota ASV richness and evenness both declined in winter compared with summer. Remarkably, the ASV richness of Nantou and Puli increased in fall compared with spring, while the evenness didn't have much difference (Fig. 3a). Generally, there were no significant differences in both Chao1 and Shannon indices at the host species level. Out of all the batches, only Fall of Puli demonstrates variation amongst host species, with *C. fargesii* having the highest α-diversity (Fig. 3b).

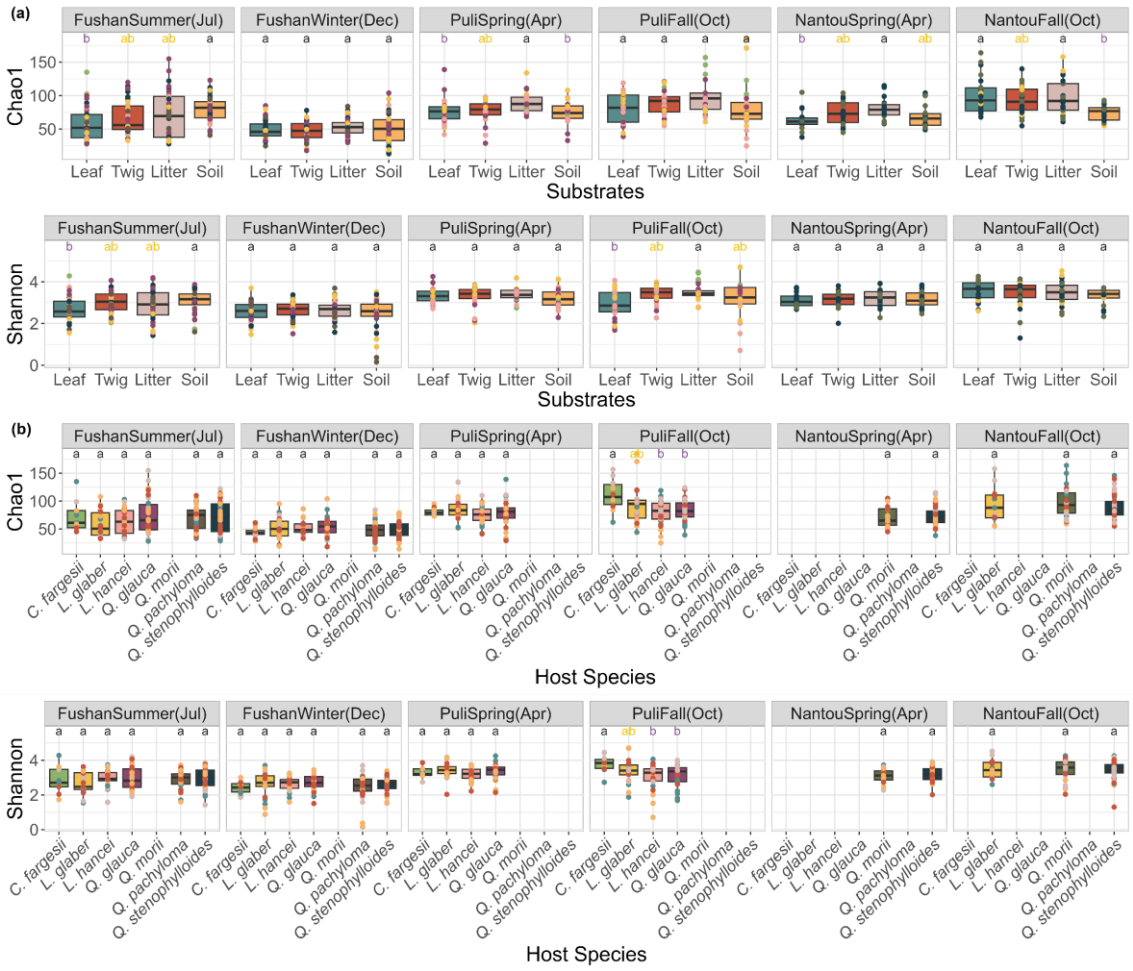

doi:10.6342/NTU202304440

Figure 3. Box plot of mycobiome α-diversity across substrates (a) and host species (b) calculated using Chao1 index and Shannon's diversity index. Sample reads were rarefied to 10,000 before estimation. The significant difference test was performed using Tukey's HSD test. Dot color in (a) represents host species and in (b) represents substrates. *C. fargesii, Castanopsis fargesii; L. glaber, Lithocarpus glaber; L. hancei, Lithocarpus hancei; Q. glauca, Quercus glauca; Q. morii, Quercus morii; Q. pachyloma, Quercus pachyloma; Q. stenophylloides, Quercus stenophylloides*.

The fungal composition differences were estimated by Bray-Curtis distance and Aitchison distance, ordinated using Non-metric Multidimensional Scaling (NMDS) analysis and Principal Co-ordinates Analysis (PCoA), respectively, while the PCoA analysis performed 13.7% of the data (Fig. 4). Both the NMDS and PCoA analyses showed that samples from the same collection location but different seasons were clustered into the same group, and statistical analyses demonstrated the significance of differences (ANOSIM R=0.4729, $p < 0.001$) between seasons. Among substrates, NMDS distance analysis showed significant distinctions between soil and the other three compartments (ANOSIM R = 0.3236, $p < 0.001$) (Fig. 4a). Interestingly, the host species has a significant but minor influence on fungal composition (ANOSIM R = 0.177, $p < 0.001$). Although the altitudes of Yilan Fushan (625-660 m) and Nantou Puli (593-774 m) were close, samples from these survey sites still clustered into separate groupings. Compared to samples from low altitudes (under 800 m), the composition of fungi on litter samples from high altitudes (over 1500 m) was more similar to soil (Fig. 4b). The results revealed that the forest mycobiome composition was most affected by the host tree's location, followed by substrates, season, and host species.

doi:10.6342/NTU202304440

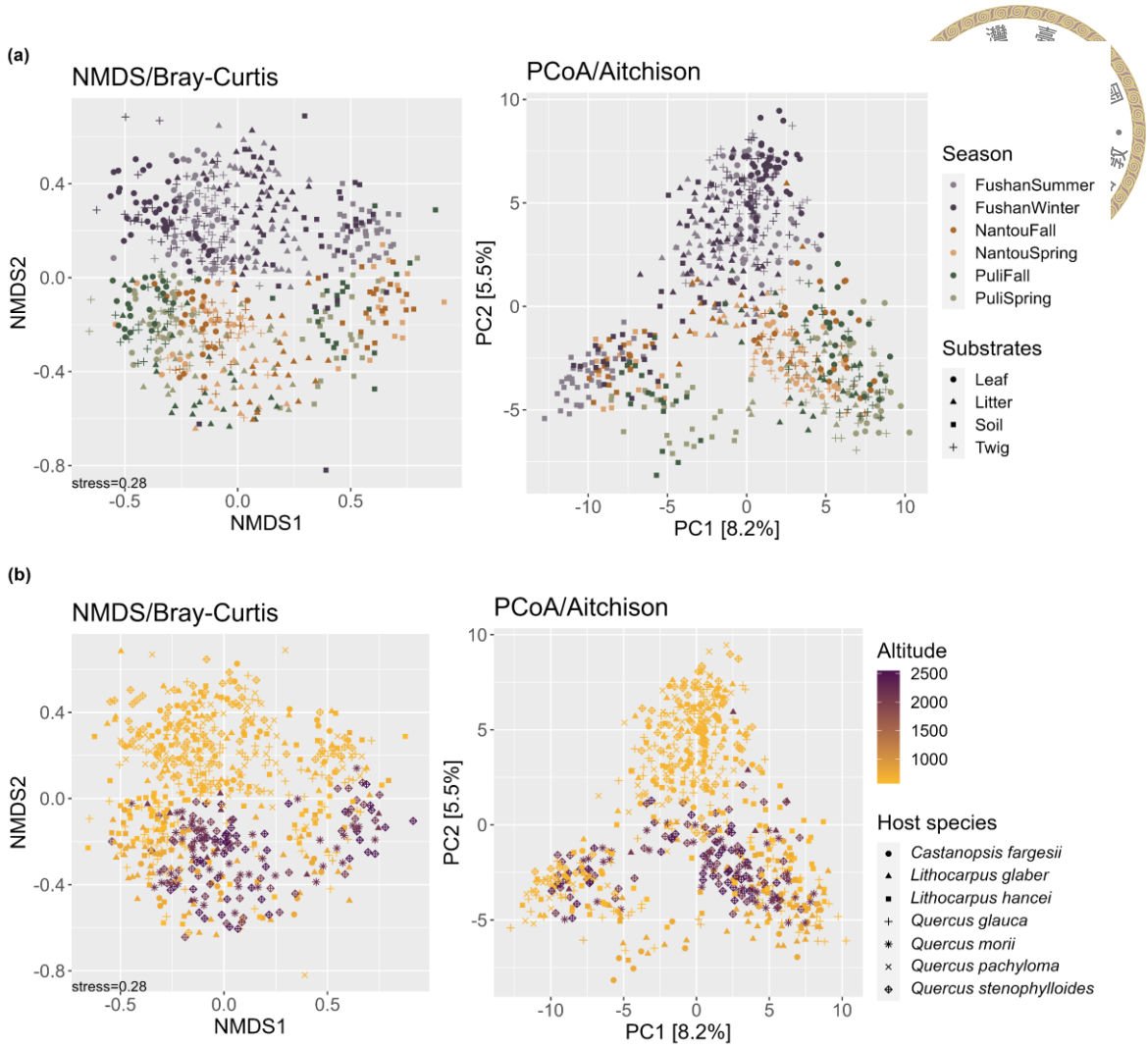

Figure 4. Mycobiota composition differences among seasons, substrates, host species, and locations. The plots were calculated using the Bray-Curtis distance and Aitchison distance, ordinated using Non-metric Multidimensional Scaling (NMDS) analysis and Principal Co-ordinates Analysis (PCoA), respectively. Samples with less than 5,000 reads were discarded before analysing. The ASVs were merged by genus. The PCoA plot can interpret 13.7% of the data. (a) The shapes represent the compartment of the sample. The colors indicate the batch of the samples; (b) The shapes represent the host species and the colors represent the altitudes (meters) of the samples.

doi:10.6342/NTU202304440

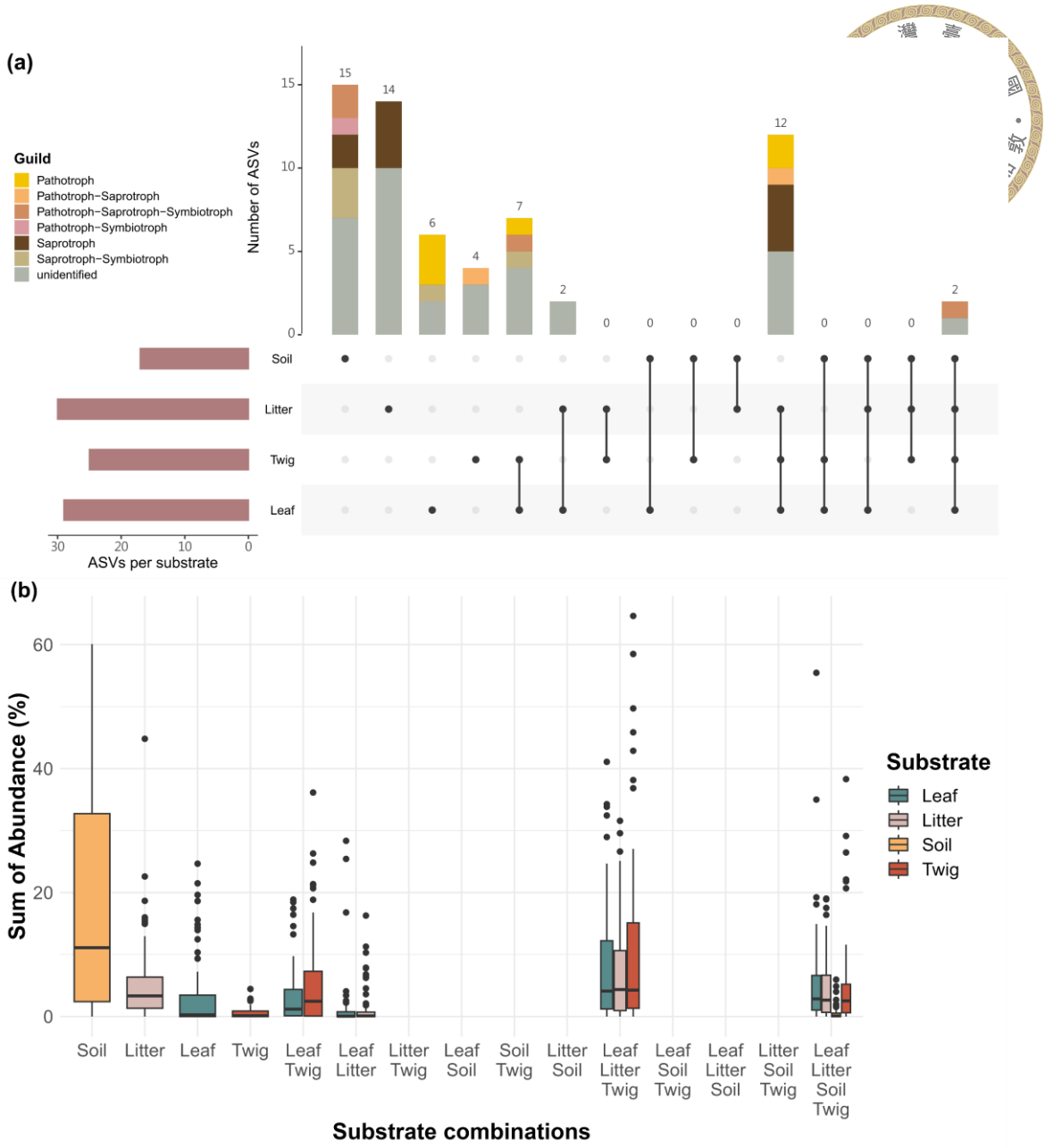

Figure 5. Number (a) and relative abundance (b) of endemic and ubiquitous ASVs among compartments. (a) The bar color indicates the guild of the ASVs; (b) Each dot represents the sum of the endemic/ubiquitous ASV abundances in one sample. The color represents the compartment.

To understand the characteristics of ASVs in each compartment, we visualized the endemic and ubiquitous ASVs in Fig. 5. In comparison to other substrates, soil contains the highest number of endemic ASVs, with the most prevalent functional guild

doi:10.6342/NTU202304440

saprotroph-symbiotroph having an average relative abundance of 3.43% across all soil samples. Surprisingly, soil and litter didn't share any ASV under our filter conditions, despite their physical proximity. There were only two ASVs that were discovered to be ubiquitous among compartments, *Cladosporium* and *Pyrenochaetopsis*, with unclassified species and no significant niche preference. Phyllosphere, including leaf, twig, and litter, shared 12 ASVs, accounting for 5% of the relative abundance in each sample (Fig. 5b; Fig. S2). The majority of the pathogenic fungi were found in aboveground substrates, where leaves had the highest abundances.

3.2 Biological replicate consistency of the forest mycobiome

To understand the representativeness of each biological replicate to the respective sample, we used the Bray-Curtis dissimilarity index to calculate the consistency between replicates (Fig. 6). Among substrates and batches, the medians of Bray-Curtis dissimilarity indices are all greater than 0.6, namely most of the samples showed a little sharing in fungal ASV composition even between biological replicates. Soil exhibits the most dissimilarity across replicates in all batches except for Fushan Summer. Among replicates, leaf has the lowest dissimilarity across seasons, suggesting that leaf might have a more stable mycobiome composition in the same tree. However, we were unable to find any significant host or climatic factor that is associated with the seasonal variations in replicate consistency.

doi:10.6342/NTU202304440

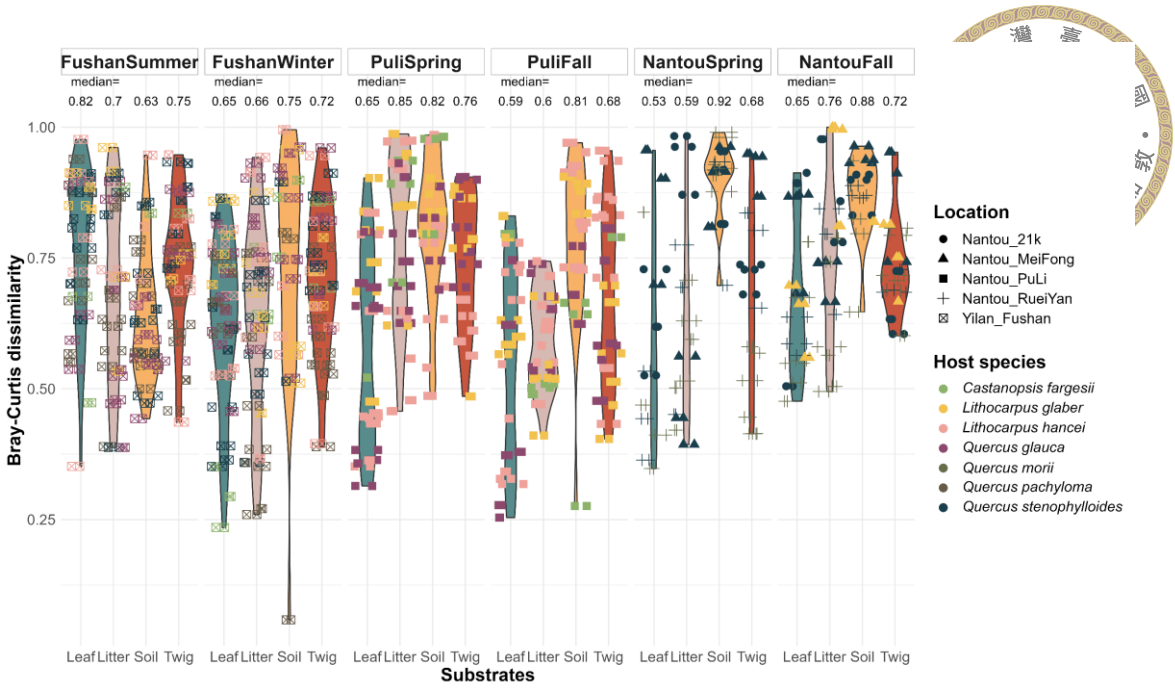

Figure 6. The biological replicates consistency among batches and compartments. The plot is estimated using the Bray-Curtis dissimilarity index. All of the samples were rarefied into 5,000 reads per sample before analysis. Each point represents the index between a pair of replicates. The color of the point denotes host species and the shape denotes locations.

3.3 Effects of abiotic factor on forest mycobiome

As season serves as a strong driver of mycobiome composition, we further look into the influence of climatic variables on mycobiome. Among relative humidity, temperature and precipitation, we found that the mycobiome composition is more likely to be affected by monthly precipitation than other climatic factors (PERMANOVA $F_{1,502}$=12.695, R^2 = 0.018, $p < 0.001$). In mycobiome composition analysis, which was estimated using Bray-Curtis distance and ordinated using PCoA, PC1 (8.1%) separated soil samples from other three compartments, while PC2 (4.9%) separated samples from high monthly precipitation to low monthly precipitation (Fig. 7). Notably, daily

doi:10.6342/NTU202304440

precipitation didn't show strong effects as monthly precipitation on fungal composition (PERMANOVA $F_{1,502}$=4.902, R^2 = 0.007, p < 0.001), indicating that the fungal composition differences are not an instant and short-lived process, but a gradual change influenced by prolonged rains.

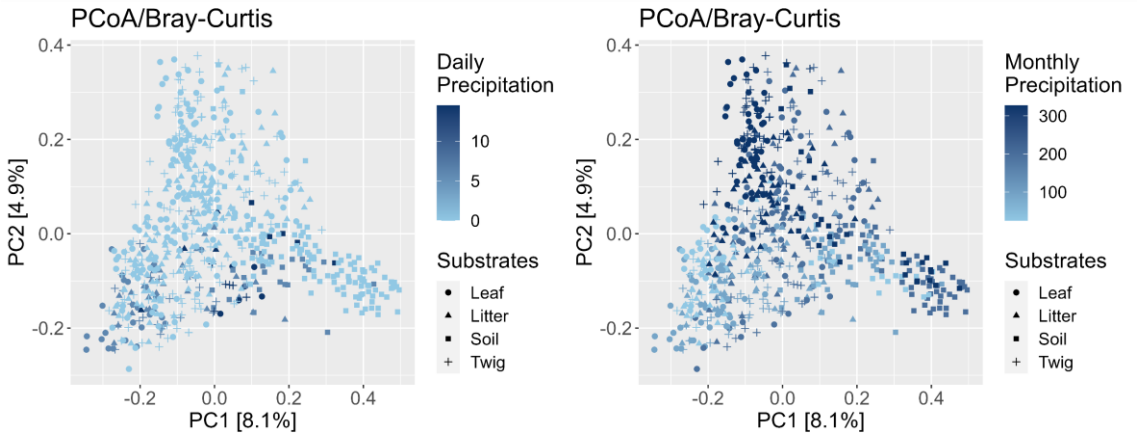

Figure 7. Variations in mycobiome composition due to monthly precipitation. The plots were calculated using the Bray-Curtis distance and were ordinated using Principal Co-ordinates Analysis (PCoA). Samples were rarefied into 5,000 reads per sample before analysing. The ASVs were merged by genus. The PCoA plot can interpret 13.0% of the data. The color represents daily (left) or monthly (right) precipitation. The shape denotes substrates.

doi:10.6342/NTU202304440

3.4 Co-occurrence network analysis and putative keystone species

The co-occurrence network of rarefied data was constructed based on 1,313,817 sequences representing 517 prevalence ASVs. The analysis revealed the influence of compartment niches on fungal complexity and connectivity (Fig. 8; Fig. S3). The network size and complexity of soil are significantly smaller than that of the other three compartments, with an average of 14 ASVs as opposed to 39 ASVs for the other three. Surprisingly, Fushan, the only artificial forest in our study, owns a significantly lower network size and complexity than the other two natural forests, indicating that an artificial forest mycobiome cannot accurately represent the actual fungal-fungal interaction in the natural environment. In comparison at the season level, the complexity of co-occurrence is disrupted in winter compared to summer in Yilan Fushan. As well, the overall complexity of the network in Puli is significantly higher than that of Nantou, suggesting that a warmer place owns a more stable network compared to a colder place. Modularity of leaf, litter and twig increase from summer to winter in Fushan, while soil decreased. In general, the modularity of the cross-module correlation of leaf increases from spring to fall, while litter decreases, twig and soil remain unchanged. With regard to the proportion changes of functional guild nodes in different seasons, fall brings an increase in the proportion of saprotroph nodes in the soil as well as saprotroph and pathotroph-saprotroph nodes in litter (Fig. S4).

To detect the importance of each node in the network, we examined their connectivity within (modular hubs: $Zi > 2.5$) and between (connectors: $Pi > 0.62$) modules (Fig. S5). In our co-occurrence network analysis, we observed an absence of shared modular hubs or connectors between batches, even within the same location, and no such entities were identified in soil or during winter. Notably, in leaf networks, eight connectors were identified, including two pathotroph-saprotroph-symbiotroph

doi:10.6342/NTU202304440

connectors (Zotu9_*Pyrenochaetopsis*, Pi=0.67, and Zotu102_*Cryptococcus*, Pi=0.65) and six unidentified connectors (Zotu145_*Piskurozyma*, Pi=0.63, Zotu402_Microbotryomycetes, Pi=0.64, Zotu599_Agaricostilbomycetes, Pi=0.64, Zotu1793_Cystobasidiomycetes, Pi=0.64, Zotu1829_*Phyllozyma dimennae*, Pi=0.64, and Zotu2153_Ascomycota, Pi=0.63). Similarly, in the twig network, two connectors were detected (saprotroph Zotu572_Teichosporaceae, Pi=0.63, and pathotroph-saprotroph-symbiotroph Zotu66_Didymosphaeriaceae, Pi=0.63). The litter network exhibited nine connectors, comprising two pathotrophs (Zotu17_*Meira nashicola*, Pi=0.63 and Zotu495_*Colacogloea*, Pi=0.69), two saprotrophs (Zotu30_*Neosetophoma*, Pi=0.63 and Zotu842_*Camposporium*, Pi=0.63), two pathotroph-saprotroph (Zotu850_ Mycosphaerellaceae, Pi=0.67 and Zotu1368_*Rhodosporidiobolus ruineniae*, Pi=0.63), two pathotroph-saprotroph-symbiotroph (Zotu44_*Aureobasidium*, Pi=0.64 and Zotu47_ *Cylindrium*, Pi=0.7) and one unidentified (Zotu827_Microbotryomycetes, Pi=0.64) connectors, along with one modular hub (pathotroph Zotu614_*Dactylaria acacia*, Zi=2.57). Remarkably, among 24 environments, only one putative keystone species — Zotu1_*Cladosporium* (Pi=0.66, Zi=2.87) — was recognized as a network hub in the leaf of Puli spring. Among four compartments, connectors were identified in leaf, twig and litter of Puli in both spring and fall, whereas in Nantou and Fushan, connectors were exclusively observed in the leaf or litter, demonstrating that a warm and dry climate may lead to lower modularity, larger modules and more opportunities for discovering connectors.

doi:10.6342/NTU202304440

Figure 8. Co-occurrence networks with significant strong correlations between ASV across seasons and substrates. Spearman correlation was utilised to estimate the correlation of mycobiome in different environments. Only strong and significant correlations were graphed (|Spearman's p| $\geqq$ 0.6, false positive adjusted p-value < 0.05). The edge color represents a positive (blue) or negative (red) correlation. The node color denotes its functional guild.

doi:10.6342/NTU202304440

3.5 Finding the exact ASV of putative keystone species by long amplicon sequencing

Due to the length restriction of Illumina sequencing and the sequence conservation of ITS2 region, we are not able to identify ASV1 to the species level. This raises the question of whether the high relative abundance of ASV1 is composed of a single species or multiple species. Therefore, in order to investigate the composition of ASV1, 10 environmental samples were selected and proceed to the Nanopore long amplicon sequencing by amplifying and sequencing fungal ribosomal operon (18S V1-ITS1-5.8S-ITS2-28S D12) with a target size up to 6 kb. Following primer trimming, quality filtering, and length filtering, a total of 1,062,678 reads were retained from 3,758,731 Nanopore raw reads. We acquired 85,503 sequences after dereplication, denoising, singleton removal, and the removal of background, chimera and false-positive ASVs, ultimately identified into 43 ASVs, with an average of 21 ASVs per sample. The sequence length of ASV range from 2,665 bp to 6,050 bp, with a median of 5,334 bp. Five ASVs were classified as *Cladosporium* sp., accounting for 4.36 % to 83.98 % of the relative abundance in each sample (Fig. 9). Notably, each *Cladosporium* ASV demonstrates a percent identity of over 99.8% with the reference sequence MH047202.1 (Fig. 10).

doi:10.6342/NTU202304440

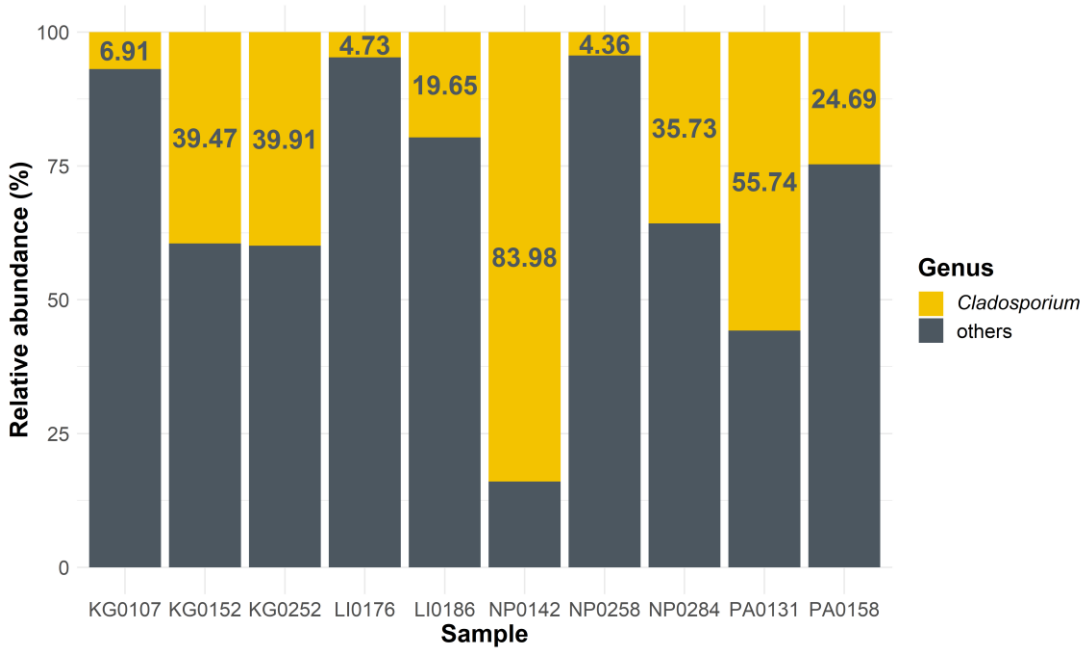

Figure 9. Relative abundance of Cladosporium in long amplicon data.

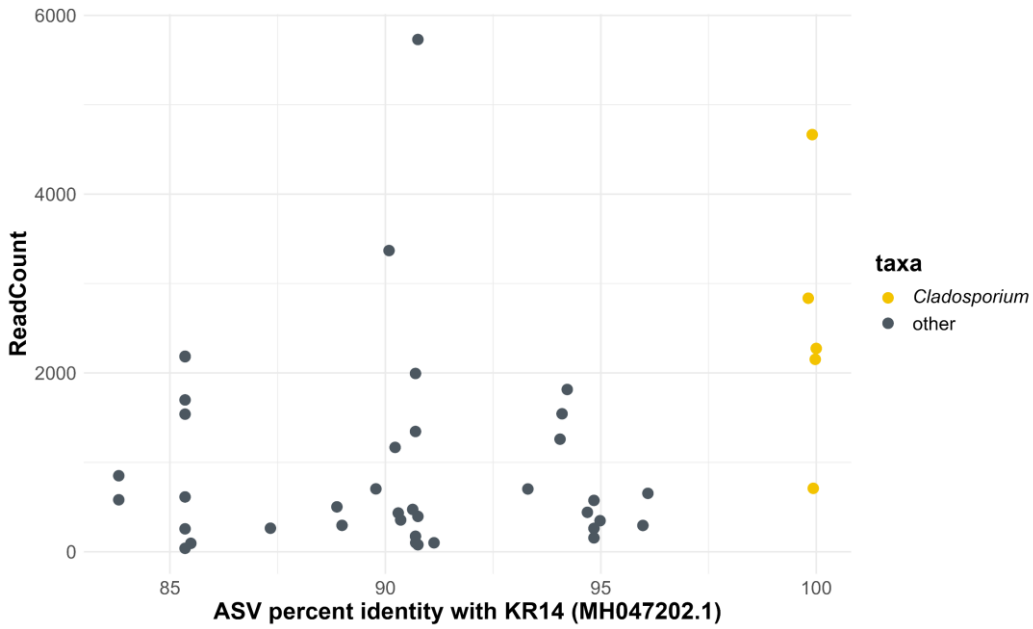

Figure 10. Percent identity of *Cladosporium* sp. strain KR14 and ASVs from long amplicon sequencing. The yellow points highlight the ASVs assigned as genus *Cladosporium*. Y-axis showed its abundance among samples.

doi:10.6342/NTU202304440

CHAPTER 4.

Discussions

. In this study, we explored the mycobiome diversity and composition of the same Fagaceae tree in two seasons to better understand the abiotic factors (such as temperature, precipitation, and humidity) and biotic factors (such as host identity and host substrates) driving the forest mycobiome. There is currently a lack of consensus regarding the substrates exhibiting higher alpha diversity since conflicting hypotheses were presented in various studies. For instance, previous studies on crop mycobiomes have indicated a higher alpha diversity in the soil compared to other substrates (Sun et al., 2021; Wei et al., 2021). Conversely, a study focused on forest mycobiomes revealed that the alpha diversity in the phyllosphere exceeded that observed in the soil compartment (Yang et al., 2022). Based on the investigation of fungal community in leaf, twig, litter, and topsoil of seven Fagaceae species of 36 trees in three Taiwanese tropical and subtropical forests, we demonstrated that the α-diversity in phyllosphere was higher than that observed in soil compartment. Interestingly, this is opposite to bacterial microbiome where α-diversity is highest in soil and low in plant phyllosphere (Thompson et al., 2017).

In contrary to the previous study, the host identity in our study didn't have a discernible impact on either α-diversity or fungal composition (Yang et al., 2022). Moreover, the results of β-diversity showed that the fungal communities in samples from high altitudes, including Nantou 21k, Nantou RenAi, Nantou ReiYan, and Nantou Meifong, were clustered together while the communities from low altitude (Yilan Fushan and Nantou Puli) didn't, suggesting that the altitude of the host location strongly shapes the fungal composition, and the mycobiome composition had a tendency of being similar along with the altitude. The biogeography pattern followed Rapoport's rule, which states

doi:10.6342/NTU202304440

that species occupying environments with greater variability in conditions are expected to have larger ecological tolerances and, consequently, larger ranges (Ogwu et al., 2019).

By comparing the results of samples from the same tree with different collecting seasons, we are able to comprehend how the mycobiome changes across two time points. The ASV richness increased in fall compared to spring, while the ASV evenness performed no evident changes, indicating that some fungal ASVs presence in autumn but none are particularly dominant. According to the β-diversity results, seasonal fluctuations serve as a significant driver of the fungal communities, especially in litter. Within the climatic variables, monthly precipitation exerts the most pronounced influence on overall fungal diversity, encompassing both mycobiome composition and richness, while daily precipitation demonstrates no significant impact on fungal diversity. The pattern aligns with findings from previous study on soil mycobiomes, where long-term precipitation emerged as the predominant factor of total fungal diversity (Bahram et al., 2018; Tedersoo et al., 2014)

The metabarcoding technique enables us to access the whole community from a single sample. However, the heterogeneity of the targeted organism in the overall environment can inherently bias the view of the community composition (Creer et al., 2016; Taberlet et al., 2012). By amplifying and sequencing the triplicate separately, we are able to understand the heterogeneity and the sample representativeness of the forest samples. The results showed that there is only a little sharing in even between the biological replicates of a single sample, which highlights the importance of sample size and the possible impact of sampling bias on ecological research. Within the substrates we collected, a more stable mycobiome composition was observed on leaf, suggesting leaf could serve as a suitable material for forest fungal investigation.

doi:10.6342/NTU202304440

In the process of data manipulation, we found that there's a high variation of false positive ASV amount in positive control by using different denoising models. Unfortunately, none of them can produce an exactly correct output, which could be caused by PCR mutation, sequencing error, chimera, or contamination (Ficetola et al., 2016). By applying a known species DNA as the positive control, we are able to find a proper data processing pipeline and threshold. That is, to gain a credible result to describe the biodiversity of the area, it is indispensable to utilize positive control in the metabarcoding approach.

We identified *Cladosporium* sp. KR14 as the keystone ASV of our study based on the combination of Illumina short amplicon and Nanopore long amplicon sequencing. The original strain was isolated from an aquatic environment in Germany (Heeger et al., 2018). A follow-up study of the strain showed its degradation ability on various humus, including laccase, lignin, triarylmethane, etc. (Rojas-Jimenez et al., 2017). The finding aligns with our results of its high abundance of leaf, litter and twig. The ASV warrants future fungus-fungus interaction studies to confirm the actual role it plays in the forests.

doi:10.6342/NTU202304440

References

Abarenkov, K., Henrik Nilsson, R., Larsson, K., Alexander, I. J., Eberhardt, U., Erland, S., Høiland, K., Kjøller, R., Larsson, E., Pennanen, T., Sen, R., Taylor, A. F. S., Tedersoo, L., Ursing, B. M., Vrålstad, T., Liimatainen, K., Peintner, U., & Kõljalg, U. (2010). The UNITE database for molecular identification of fungi – recent updates and future perspectives. *New Phytologist*, *186*(2), 281–285. https://doi.org/10.1111/j.1469-8137.2009.03160.x

Aydogan, E. L., Moser, G., Müller, C., Kämpfer, P., & Glaeser, S. P. (2018). Long-Term Warming Shifts the Composition of Bacterial Communities in the Phyllosphere of *Galium album* in a Permanent Grassland Field-Experiment. *Frontiers in Microbiology*, *9*. https://doi.org/10.3389/fmicb.2018.00144

Bahram, M., Hildebrand, F., Forslund, S. K., Anderson, J. L., Soudzilovskaia, N. A., Bodegom, P. M., Bengtsson-Palme, J., Anslan, S., Coelho, L. P., Harend, H., Huerta-Cepas, J., Medema, M. H., Maltz, M. R., Mundra, S., Olsson, P. A., Pent, M., Põlme, S., Sunagawa, S., Ryberg, M., … Bork, P. (2018). Structure and function of the global topsoil microbiome. *Nature*, *560*(7717), 233–237. https://doi.org/10.1038/s41586-018-0386-6

Bai, Y., Kissoudis, C., Yan, Z., Visser, R. G. F., & van der Linden, G. (2018). Plant behaviour under combined stress: tomato responses to combined salinity and pathogen stress. *The Plant Journal*, *93*(4), 781–793. https://doi.org/10.1111/tpj.13800

Baldrian, P. (2017). Forest microbiome: Diversity, complexity and dynamics. *FEMS Microbiology Reviews*, *41*(2), 109–130. https://doi.org/10.1093/femsre/fuw040

doi:10.6342/NTU202304440

Baldrian, P., López-Mondéjar, R., & Kohout, P. (2023). Forest microbiome and global change. *Nature Reviews Microbiology, 21*(8), 487–501. *Nature Research*. https://doi.org/10.1038/s41579-023-00876-4

Bengtsson-Palme, J., Ryberg, M., Hartmann, M., Branco, S., Wang, Z., Godhe, A., De Wit, P., Sánchez-García, M., Ebersberger, I., de Sousa, F., Amend, A., Jumpponen, A., Unterseher, M., Kristiansson, E., Abarenkov, K., Bertrand, Y. J. K., Sanli, K., Eriksson, K. M., Vik, U., … Nilsson, R. H. (2013). Improved software detection and extraction of ITS1 and ITS2 from ribosomal ITS sequences of fungi and other eukaryotes for analysis of environmental sequencing data. *Methods in Ecology and Evolution*, *4*(10), 914–919. https://doi.org/10.1111/2041-210X.12073

Blaalid, R., Kumar, S., Nilsson, R. H., Abarenkov, K., Kirk, P. M., & Kauserud, H. (2013). ITS1 versus ITS2 as DNA metabarcodes for fungi. *Molecular Ecology Resources*, *13*(2), 218–224. https://doi.org/10.1111/1755-0998.12065

Bolyen, E., Rideout, J. R., Dillon, M. R., Bokulich, N. A., Abnet, C. C., Al-Ghalith, G. A., Alexander, H., Alm, E. J., Arumugam, M., Asnicar, F., Bai, Y., Bisanz, J. E., Bittinger, K., Brejnrod, A., Brislawn, C. J., Brown, C. T., Callahan, B. J., Caraballo-Rodríguez, A. M., Chase, J., … Caporaso, J. G. (2019). Reproducible, interactive, scalable and extensible microbiome data science using QIIME 2. *Nature Biotechnology*, *37*(8), 852–857. https://doi.org/10.1038/s41587-019-0209-9

Camacho, C., Coulouris, G., Avagyan, V., Ma, N., Papadopoulos, J., Bealer, K., & Madden, T. L. (2009). BLAST+: architecture and applications. *BMC Bioinformatics*, *10*(1), 421. https://doi.org/10.1186/1471-2105-10-421

doi:10.6342/NTU202304440

Chamberlain, S. A., & Boettiger, C. (2017). R Python, and Ruby clients for GBIF species occurrence data. *PeerJ Preprints*, *5*, e3304v1. https://doi.org/https://doi.org/10.7287/peerj.preprints.3304v1

Chen, S., Zhou, Y., Chen, Y., & Gu, J. (2018). fastp: an ultra-fast all-in-one FASTQ preprocessor. *Bioinformatics*, *34*(17), i884–i890. https://doi.org/10.1093/bioinformatics/bty560

Creer, S., Deiner, K., Frey, S., Porazinska, D., Taberlet, P., Thomas, W. K., Potter, C., & Bik, H. M. (2016). The ecologist's field guide to sequence-based identification of biodiversity. *Methods in Ecology and Evolution, 7*(9), pp. 1008–1018). British Ecological Society. https://doi.org/10.1111/2041-210X.12574

Csardi, G., & Nepusz, T. (2006). The igraph software package for complex network research. *InterJournal, Complex Systems*, *1695*(5), 1–9.

D'Andreano, S., Cuscó, A., & Francino, O. (2021). Rapid and real-Time identification of fungi up to species level with long amplicon nanopore sequencing from clinical samples. *Biology Methods and Protocols*, *6*(1). https://doi.org/10.1093/biomethods/bpaa026

Edgar, R. C. (2013). UPARSE: Highly accurate OTU sequences from microbial amplicon reads. *Nature Methods*, *10*(10), 996–998. https://doi.org/10.1038/nmeth.2604

Edgar, R. C. (2016). UNOISE2: improved error-correction for Illumina 16S and ITS amplicon sequencing. *BioRxiv*. https://doi.org/10.1101/081257

Ehrenberg, R. (2015). Global forest survey finds trillions of trees. *Nature, 525*(7568), 170-171. https://doi.org/10.1038/nature.2015.18287

doi:10.6342/NTU202304440

Ficetola, G. F., Taberlet, P., & Coissac, E. (2016). How to limit false positives in environmental DNA and metabarcoding? *Molecular Ecology Resources*, *16*(3), 604–607. https://doi.org/10.1111/1755-0998.12508

Friedman, J., & Alm, E. J. (2012). Inferring Correlation Networks from Genomic Survey Data. *PLoS Computational Biology*, *8*(9), e1002687. https://doi.org/10.1371/journal.pcbi.1002687

Garnica, S., Schön, M. E., Abarenkov, K., Riess, K., Liimatainen, K., Niskanen, T., Dima, B., Soop, K., Frøslev, T. G., Jeppesen, T. S., Peintner, U., Kuhnert-Finkernagel, R., Brandrud, T. E., Saar, G., Oertel, B., & Ammirati, J. F. (2016). Determining threshold values for barcoding fungi: lessons from *Cortinarius* (Basidiomycota), a highly diverse and widespread ectomycorrhizal genus. *FEMS Microbiology Ecology*, *92*(4), fiw045. https://doi.org/10.1093/femsec/fiw045

Heeger, F., Bourne, E. C., Baschien, C., Yurkov, A., Bunk, B., Spröer, C., Overmann, J., Mazzoni, C. J., & Monaghan, M. T. (2018). Long-read DNA metabarcoding of ribosomal RNA in the analysis of fungi from aquatic environments. *Molecular Ecology Resources*, *18*(6), 1500–1514. https://doi.org/10.1111/1755-0998.12937

Hoang, M. T. V., Irinyi, L., Chen, S. C. A., Sorrell, T. C., & Meyer, W. (2019). Dual DNA Barcoding for the Molecular Identification of the Agents of Invasive Fungal Infections. *Frontiers in Microbiology*, *10*. https://doi.org/10.3389/fmicb.2019.01647

Kauserud, H. (2023). ITS alchemy: On the use of ITS as a DNA marker in fungal ecology. *Fungal Ecology*, *65*, 101274. https://doi.org/10.1016/j.funeco.2023.101274

doi:10.6342/NTU202304440

Koch, A., & Kaplan, J. O. (2022). Tropical forest restoration under future climate change. *Nature Climate Change*, *12*(3), 279–283. https://doi.org/10.1038/s41558-022-01289-6

Łaźniewska, J., Macioszek, V. K., & Kononowicz, A. K. (2012). Plant-fungus interface: The role of surface structures in plant resistance and susceptibility to pathogenic fungi. *Physiological and Molecular Plant Pathology*, *78*, 24–30. https://doi.org/10.1016/j.pmpp.2012.01.004

Lee, T. J., Liu, Y. C., Liu, W. A., Lin, Y. F., Lee, H. H., Ke, H. M., Huang, J. P., Lu, M. Y. J., Hsieh, C. L., Chung, K. F., Liti, G., & Tsai, I. J. (2022). Extensive sampling of *Saccharomyces cerevisiae* in Taiwan reveals ecology and evolution of predomesticated lineages. *Genome Research*, *32*(5), 864–877. https://doi.org/10.1101/gr.276286.121

Leveau, J. H. (2019). A brief from the leaf: latest research to inform our understanding of the phyllosphere microbiome. *Current Opinion in Microbiology*, *49*, 41–49. https://doi.org/10.1016/j.mib.2019.10.002

Li, C., Chytrý, M., Zelený, D., Chen, M., Chen, T., Chiou, C., Hsia, Y., Liu, H., Yang, S., Yeh, C., Wang, J., Yu, C., Lai, Y., Chao, W., & Hsieh, C. (2013). Classification of Taiwan forest vegetation. *Applied Vegetation Science*, *16*(4), 698–719. https://doi.org/10.1111/avsc.12025

Liber, J. A., Bonito, G., & Benucci, G. M. N. (2021). CONSTAX2: improved taxonomic classification of environmental DNA markers. *Bioinformatics*, *37*(21), 3941–3943. https://doi.org/10.1093/bioinformatics/btab347

Lin, J.-C., Chiou, C.-R., Chan, W.-H., & Wu, M.-S. (2021). Valuation of Forest Ecosystem Services in Taiwan. *Forests*, *12*(12), 1694. https://doi.org/10.3390/f12121694

doi:10.6342/NTU202304440

Liu, S., García-Palacios, P., Tedersoo, L., Guirado, E., van der Heijden, M. G. A., Wagg, C., Chen, D., Wang, Q., Wang, J., Singh, B. K., & Delgado-Baquerizo, M. (2022). Phylotype diversity within soil fungal functional groups drives ecosystem stability. *Nature Ecology and Evolution*, *6*(7), 900–909. https://doi.org/10.1038/s41559-022-01756-5

Martin, M. (2011). Cutadapt removes adapter sequences from high-throughput sequencing reads. *EMBnet.Journal*, *17*(1), 10. https://doi.org/10.14806/ej.17.1.200

McMurdie, P. J., & Holmes, S. (2013). Phyloseq: An R Package for Reproducible Interactive Analysis and Graphics of Microbiome Census Data. *PLoS ONE*, *8*(4). https://doi.org/10.1371/journal.pone.0061217

Meiser, A., Bálint, M., & Schmitt, I. (2014). Meta-analysis of deep-sequenced fungal communities indicates limited taxon sharing between studies and the presence of biogeographic patterns. *New Phytologist*, *201*(2), 623–635. https://doi.org/10.1111/nph.12532

Nguyen, N. H., Song, Z., Bates, S. T., Branco, S., Tedersoo, L., Menke, J., Schilling, J. S., & Kennedy, P. G. (2016). FUNGuild: An open annotation tool for parsing fungal community datasets by ecological guild. *Fungal Ecology*, *20*, 241–248. https://doi.org/10.1016/j.funeco.2015.06.006

Ogwu, M. C., Takahashi, K., Dong, K., Song, H. K., Moroenyane, I., Waldman, B., & Adams, J. M. (2019). Fungal Elevational Rapoport pattern from a High Mountain in Japan. *Scientific Reports*, *9*(1). https://doi.org/10.1038/s41598-019-43025-9

doi:10.6342/NTU202304440

Peay, K. G., Kennedy, P. G., & Talbot, J. M. (2016). Dimensions of biodiversity in the Earth mycobiome. *Nature Reviews Microbiology*, *14*(7), 434–447. https://doi.org/10.1038/nrmicro.2016.59

Rojas-Jimenez, K., Fonvielle, J. A., Ma, H., & Grossart, H. P. (2017). Transformation of humic substances by the freshwater Ascomycete *Cladosporium* sp. *Limnology and Oceanography*, *62*(5), 1955–1962. https://doi.org/10.1002/lno.10545

Rosier, A., Bishnoi, U., Lakshmanan, V., Sherrier, D. J., & Bais, H. P. (2016). A perspective on inter-kingdom signaling in plant–beneficial microbe interactions. *Plant Molecular Biology*, *90*(6), 537–548. https://doi.org/10.1007/s11103-016-0433-3

RStudio Team. (2020). *RStudio: Integrated Development Environment for R*. RStudio, PBC.

Sasse, J., Martinoia, E., & Northen, T. (2018). Feed Your Friends: Do Plant Exudates Shape the Root Microbiome? *Trends in Plant Science*, *23*(1), 25–41. https://doi.org/10.1016/j.tplants.2017.09.003

Sayers, E. W., Bolton, E. E., Brister, J. R., Canese, K., Chan, J., Comeau, D. C., Connor, R., Funk, K., Kelly, C., Kim, S., Madej, T., Marchler-Bauer, A., Lanczycki, C., Lathrop, S., Lu, Z., Thibaud-Nissen, F., Murphy, T., Phan, L., Skripchenko, Y., … Sherry, S. T. (2022). Database resources of the national center for biotechnology information. *Nucleic Acids Research*, *50*(D1), D20–D26. https://doi.org/10.1093/nar/gkab1112

Schiro, G., Verch, G., Grimm, V., & Müller, M. (2018). *Alternaria* and *Fusarium* Fungi: Differences in Distribution and Spore Deposition in a Topographically

doi:10.6342/NTU202304440

Heterogeneous Wheat Field. *Journal of Fungi*, *4*(2), 63. https://doi.org/10.3390/jof4020063

Stone, B. W. G., Weingarten, E. A., & Jackson, C. R. (2018). The role of the phyllosphere microbiome in plant health and function. *Annual Plant Reviews Online*, *1*(2), 533–556. https://doi.org/10.1002/9781119312994.apr0614

Syed Ab Rahman, S. F., Singh, E., Pieterse, C. M. J., & Schenk, P. M. (2018). Emerging microbial biocontrol strategies for plant pathogens. *Plant Science*, *267*, 102–111. https://doi.org/10.1016/j.plantsci.2017.11.012

Taberlet, P., Prud'Homme, S. M., Campione, E., Roy, J., Miquel, C., Shehzad, W., Gielly, L., Rioux, D., Choler, P., Clément, J., Melodelima, C., Pompanon, F., & Coissac, E. (2012). Soil sampling and isolation of extracellular DNA from large amount of starting material suitable for metabarcoding studies. *Molecular Ecology*, *21*(8), 1816–1820. https://doi.org/10.1111/j.1365-294X.2011.05317.x

Tedersoo, L., Anslan, S., Bahram, M., Põlme, S., Riit, T., Liiv, I., Kõljalg, U., Kisand, V., Nilsson, R. H., Hildebrand, F., Bork, P., & Abarenkov, K. (2015). Shotgun metagenomes and multiple primer pair-barcode combinations of amplicons reveal biases in metabarcoding analyses of fungi. *MycoKeys*, *10*, 1–43. https://doi.org/10.3897/mycokeys.10.4852

Tedersoo, L., Bahram, M., Põlme, S., Kõljalg, U., Yorou, N. S., Wijesundera, R., Ruiz, L. V., Vasco-Palacios, A. M., Thu, P. Q., Suija, A., Smith, M. E., Sharp, C., Saluveer, E., Saitta, A., Rosas, M., Riit, T., Ratkowsky, D., Pritsch, K., Põldmaa, K., … Abarenkov, K. (2014). Global diversity and geography of soil fungi. *Science, 346(*6213). https://doi.org/10.1126/science.1256688

doi:10.6342/NTU202304440

Tedersoo, L., & Lindahl, B. (2016). Fungal identification biases in microbiome projects. *Environmental Microbiology Reports*, *8*(5), 774–779. https://doi.org/10.1111/1758-2229.12438

Thompson, L. R., Sanders, J. G., McDonald, D., Amir, A., Ladau, J., Locey, K. J., Prill, R. J., Tripathi, A., Gibbons, S. M., Ackermann, G., Navas-Molina, J. A., Janssen, S., Kopylova, E., Vázquez-Baeza, Y., González, A., Morton, J. T., Mirarab, S., Xu, Z. Z., Jiang, L., … Zhao, H. (2017). A communal catalogue reveals Earth's multiscale microbial diversity. *Nature*, *551*(7681), 457–463. https://doi.org/10.1038/nature24621

Tomao, A., Antonio Bonet, J., Castaño, C., & de-Miguel, S. (2020). How does forest management affect fungal diversity and community composition? Current knowledge and future perspectives for the conservation of forest fungi. *Forest Ecology and Management*, *457*, 117678. https://doi.org/10.1016/j.foreco.2019.117678

Truchado, P., Gil, M. I., Moreno-Candel, M., & Allende, A. (2019). Impact of weather conditions, leaf age and irrigation water disinfection on the major epiphytic bacterial genera of baby spinach grown in an open field. *Food Microbiology*, *78*, 46–52. https://doi.org/10.1016/j.fm.2018.09.015

Vilgalys lab. (1992). *Conserved primer sequences for PCR amplification and sequencing from nuclear ribosomal RNA*. https://sites.duke.edu/vilgalyslab/files/2017/08/rDNA-primers-for-fungi.pdf

Villanueva, R. A. M., & Chen, Z. J. (2019). ggplot2: Elegant Graphics for Data Analysis (2nd ed.). *Measurement: Interdisciplinary Research and Perspectives*, *17*(3), 160–167. https://doi.org/10.1080/15366367.2019.1565254

doi:10.6342/NTU202304440

Wagg, C., Schlaeppi, K., Banerjee, S., Kuramae, E. E., & van der Heijden, M. G. A. (2019). Fungal-bacterial diversity and microbiome complexity predict ecosystem functioning. *Nature Communications*, *10*(1). https://doi.org/10.1038/s41467-019-12798-y

Watts, S. C., Ritchie, S. C., Inouye, M., & Holt, K. E. (2019). FastSpar: rapid and scalable correlation estimation for compositional data. *Bioinformatics*, *35*(6), 1064–1066. https://doi.org/10.1093/bioinformatics/bty734

Yan, L., Zhu, J., Zhao, X., Shi, J., Jiang, C., & Shao, D. (2019). Beneficial effects of endophytic fungi colonization on plants. *Applied Microbiology and Biotechnology*, *103*(8), 3327–3340. https://doi.org/10.1007/s00253-019-09713-2

Yang, H., Yang, Z., Wang, Q.-C., Wang, Y.-L., Hu, H.-W., He, J.-Z., Zheng, Y., & Yang, Y. (2022). Compartment and Plant Identity Shape Tree Mycobiome in a Subtropical Forest. *Microbiology Spectrum*, *10*(4). https://doi.org/10.1128/spectrum.01347-22

doi:10.6342/NTU202304440

Supplementary Materials

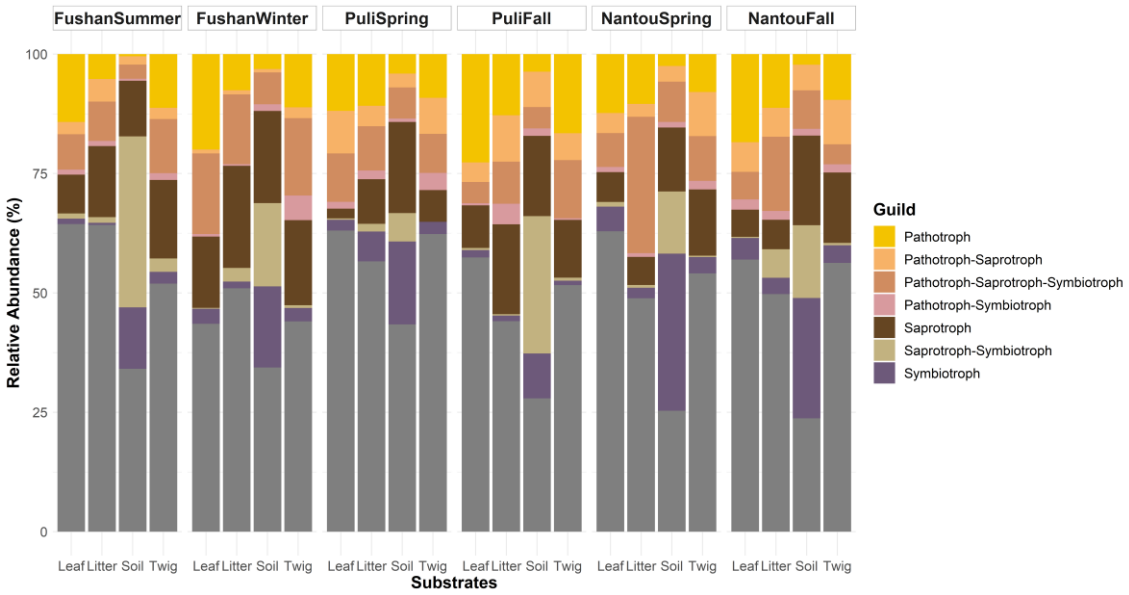

Figure S1. Bar plot of mean of guild relative abundance of unique and shared ASVs of the intersections among four compartments.

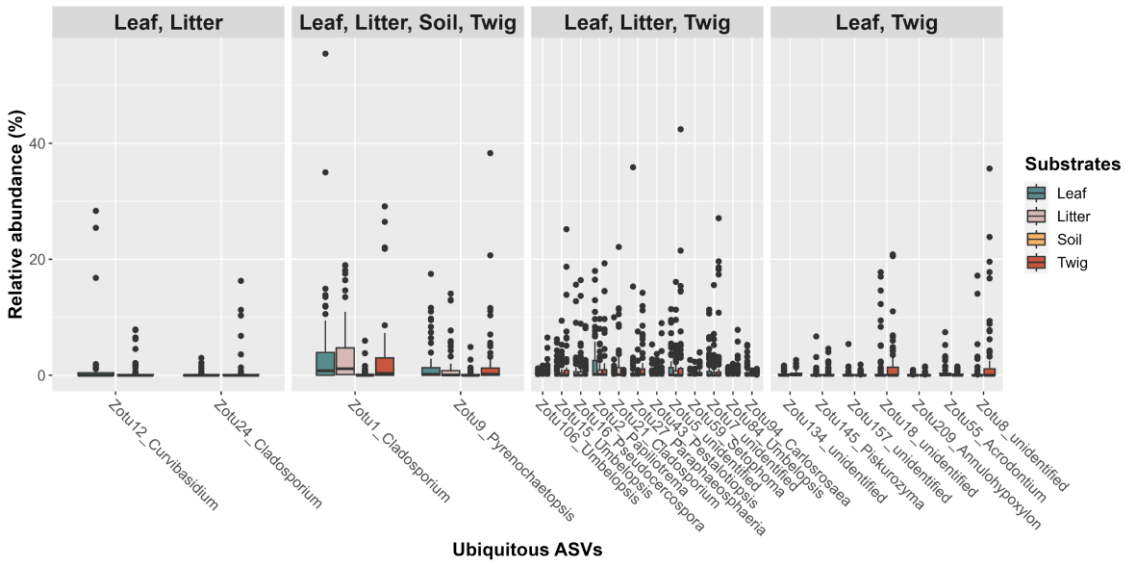

Figure S2. Relative abundance of ubiquitous ASVs among compartments.

doi:10.6342/NTU202304440

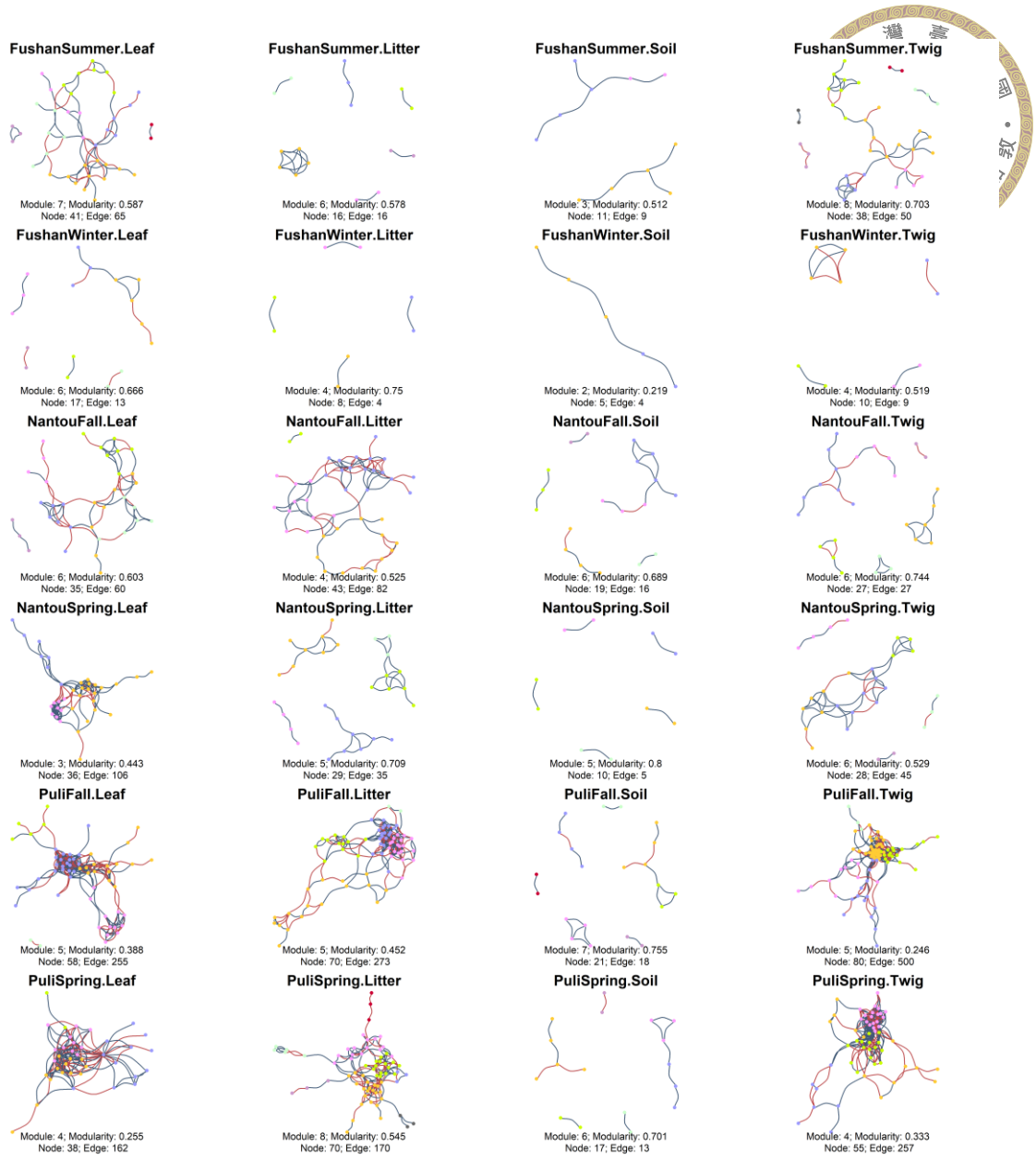

Figure S3. Co-occurrence networks illustrating robust correlations among ASVs across seasons and substrates. Spearman correlation assessed mycobiome correlation in distinct environments. Only significant and strong correlations are depicted (|Spearman's $\rho| \geq 0.6$, false-positive adjusted p-value < 0.05). Edge colors signify positive (blue) or negative (red) correlations, while node colors represent the module classification.

doi:10.6342/NTU202304440

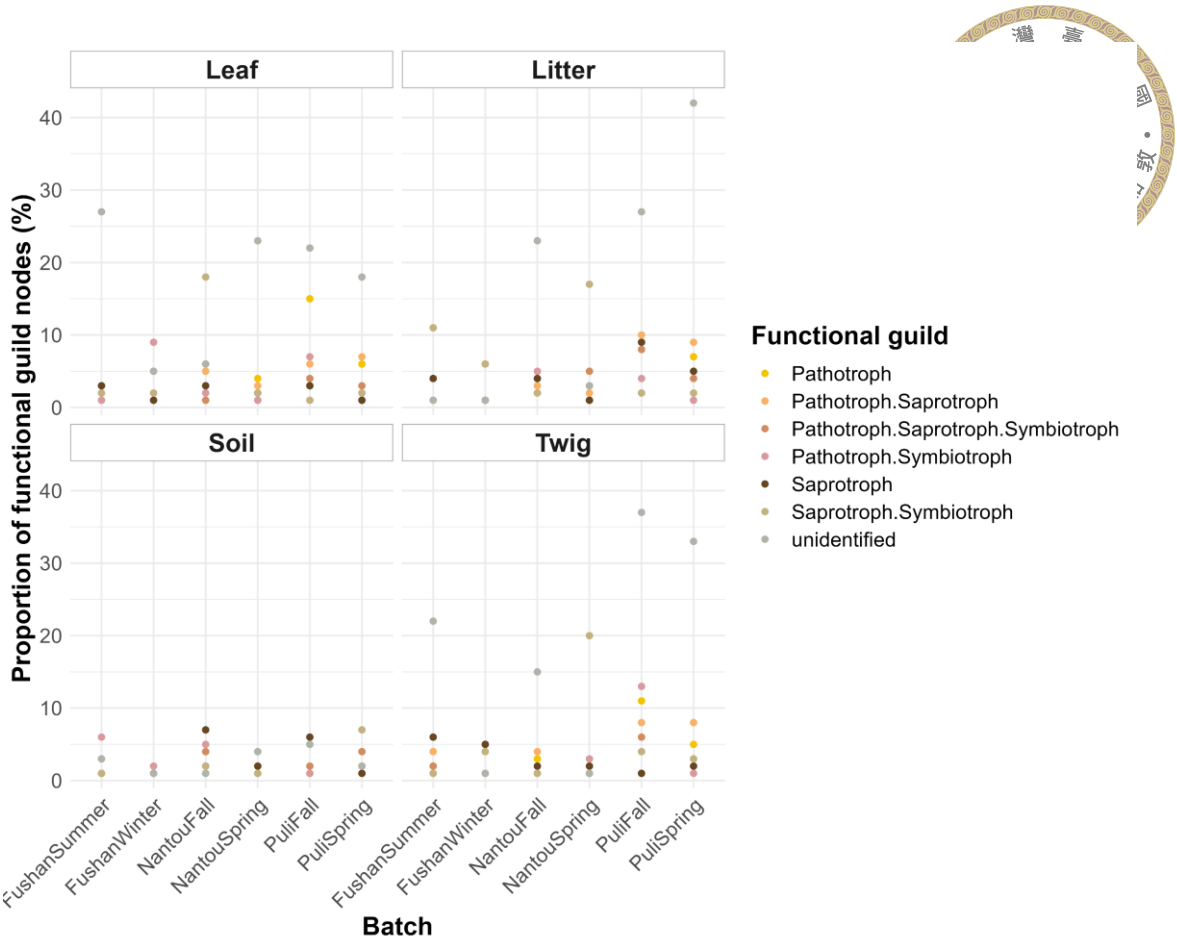

Figure S4. The proportion changes of functional guild nodes in the co-occurrence network under 24 environments. The color denotes functional guild.

doi:10.6342/NTU202304440

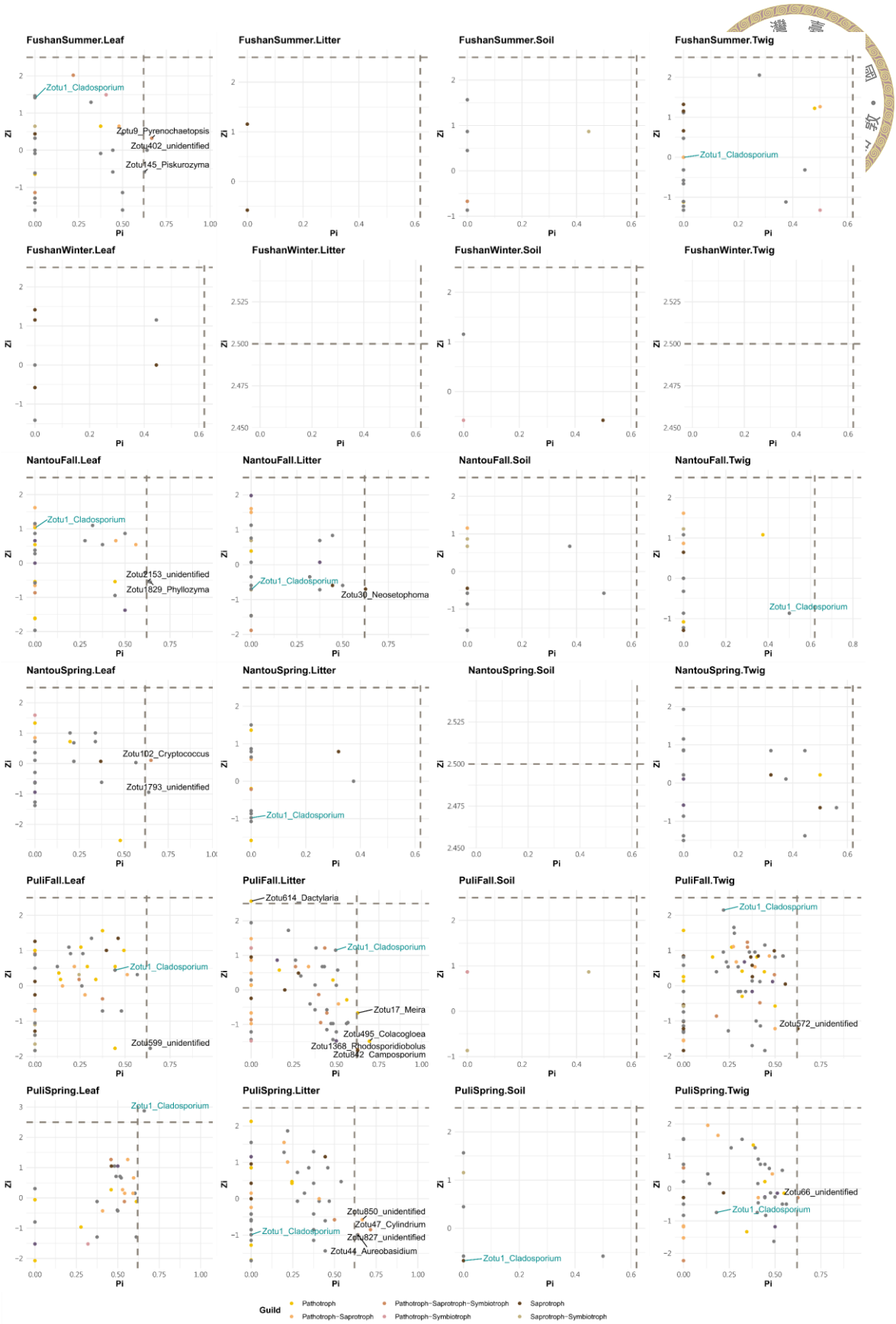

Figure S5. The connectively within and among modules of vertices in the co-occurrence network. Zi: connectivity within module; Pi: connectivity among modules.

doi:10.6342/NTU202304440

Table S1. Tree information

Tree no.	Latitude	Longitude	Altitude	Location	Scientific name	Batch	Sequencing by
SPA0281	24.09128	121.1763	2053.626	Nantou_MeiFong	*Quercus stenophylloides*	NantouSpring, NantouFall	merged
SPA0291	24.09102	121.1767	2045.293	Nantou_MeiFong	*Quercus stenophylloides*	NantouSpring, NantouFall	separated
SPA0423	24.09722	121.1808	2170.401123	Nantou_RueiYan	*Quercus stenophylloides*	NantouSpring, NantouFall	separated
SPA0424	24.09714	121.1807	2169.718994	Nantou_RueiYan	*Quercus morii*	NantouSpring, NantouFall	separated
SPA0425	24.09959	121.1808	2159.156738	Nantou_RueiYan	*Quercus morii*	NantouSpring, NantouFall	separated
SPA0428	24.11293	121.2147	2547.580566	Nantou_RenAi	*Quercus stenophylloides*	NantouSpring, NantouFall	merged
SPA0429	24.11294	121.2148	2548.802002	Nantou_RenAi	*Quercus stenophylloides*	NantouSpring, NantouFall	merged
SPA0432	24.11166	121.214	2536.202881	Nantou_21k	*Quercus stenophylloides*	NantouSpring, NantouFall	separated
SPA0440	24.11147	121.2138	2536.835205	Nantou_21k	*Quercus stenophylloides*	NantouSpring, NantouFall	merged
SPA0441	23.99013	121.0159	593.126831	Nantou_PuLi	*Quercus glauca*	PuliSpring, PuliFall	separated
SPA0442	23.9902	121.016	572.788818	Nantou_PuLi	*Quercus glauca*	PuliSpring, PuliFall	separated
SPA0443	23.99349	121.0131	584.041626	Nantou_PuLi	*Lithocarpus hancei*	PuliSpring, PuliFall	separated
SPA0444	23.99445	121.0117	623.210388	Nantou_PuLi	*Lithocarpus hancei*	PuliSpring, PuliFall	separated
SPA0445	23.99648	121.0098	746.667175	Nantou_PuLi	*Lithocarpus hancei*	PuliSpring, PuliFall	separated
SPA0446	23.99654	121.0109	757.397705	Nantou_PuLi	*Quercus glauca*	PuliSpring	separated
SPA0447	23.99631	121.0132	779.861938	Nantou_PuLi	*Lithocarpus glaber*	PuliSpring, PuliFall	separated
SPA0448	23.99642	121.0131	775.051086	Nantou_PuLi	*Lithocarpus glaber*	PuliSpring, PuliFall	separated
SPA0449	23.99646	121.0131	774.686462	Nantou_PuLi	*Castanopsis fargesii*	PuliSpring, PuliFall	separated
SPA0472	24.09	121.1739	2090.012695	Nantou_MeiFong	*Lithocarpus glaber*	NantouFall	separated
SPA0084	24.7626	121.5853	625.3	Yilan_Fushan	*Quercus pachyloma*	FushanSummer, FushanWinter	separated
SPA0086	24.7623	121.5851	638	Yilan_Fushan	*Quercus glauca*	FushanSummer, FushanWinter	separated
SPA0097	24.7621	121.5845	650.8	Yilan_Fushan	*Quercus glauca*	FushanSummer, FushanWinter	merged
SPA0104	24.7622	121.5852	649.4	Yilan_Fushan	*Lithocarpus hancei*	FushanSummer, FushanWinter	separated
SPA0326	24.7622	121.5846	651.323242	Yilan_Fushan	*Quercus glauca*	FushanSummer, FushanWinter	separated
SPA0332	24.76186	121.5841	648.798401	Yilan_Fushan	*Castanopsis fargesii*	FushanSummer, FushanWinter	separated
SPA0450	24.76224	121.5847	655.134644	Yilan_Fushan	*Lithocarpus hancei*	FushanSummer, FushanWinter	separated
SPA0451	24.7623	121.5849	657.323975	Yilan_Fushan	*Quercus glauca*	FushanSummer, FushanWinter	separated
SPA0452	24.76218	121.5851	655.921021	Yilan_Fushan	*Lithocarpus glaber*	FushanSummer, FushanWinter	separated
SPA0454	24.76282	121.5855	645.572449	Yilan_Fushan	*Quercus stenophylloides*	FushanSummer, FushanWinter	merged
SPA0455	24.76281	121.5856	658.40509	Yilan_Fushan	*Quercus stenophylloides*	FushanSummer, FushanWinter	separated
SPA0456	24.76288	121.5856	657.876648	Yilan_Fushan	*Quercus stenophylloides*	FushanSummer, FushanWinter	merged
SPA0457	24.76293	121.5856	658.087341	Yilan_Fushan	*Quercus stenophylloides*	FushanSummer	separated
SPA0458	24.76285	121.5855	659.571472	Yilan_Fushan	*Quercus stenophylloides*	FushanSummer, FushanWinter	merged
SPA0459	24.76277	121.5855	660.307617	Yilan_Fushan	*Quercus stenophylloides*	FushanSummer, FushanWinter	separated
SPA0460	24.76247	121.5852	658.571289	Yilan_Fushan	*Quercus pachyloma*	FushanSummer, FushanWinter	separated

doi:10.6342/NTU202304440

SPA0461	24.76246	121.5853	657.412292	Yilan_Fushan	*Quercus pachyloma*	FushanSummer, FushanWinter	separated
SPA0462	24.76231	121.585	651.662659	Yilan_Fushan	*Lithocarpus glaber*	FushanSummer, FushanWinter	separated
SPA0487	24.76293	121.5855	657.582825	Yilan_Fushan	*Quercus stenophylloides*	FushanWinter	separated

doi:10.6342/NTU202304440

Table S2. Survey sites weather information

Batch (Date)	Precipitation (mm)	Monthly Precipitation (mm)	Temperature (℃)	Monthly Temperature (℃)	RH (%)	Monthly RH (%)
FushanSummer (2022.7.1)	0	202	22.6	24.1	94	89
FushanWinter (2022.12.26)	0	327.5	8.3	11.9	NA	NA
NantouSpring (2022.4.18)	0	193.5	12.1	12.5	92	87
NantouSpring (2022.4.19)	14.5	193.5	11.3	12.5	99	87
NantouFall (2022.10.24)	0	90	14.3	15.1	94	85
NantouFall (2022.10.25)	0	90	13	15.1	94	85
NantouFall (2022.10.26)	0	90	13	15.1	93	85
PuliSpring (2022.4.18)	0	92	21.7	22.6	79	79
PuliSpring (2022.4.19)	6	92	20.7	22.6	88	79
PuliFall (2022.10.24)	0	25	23.4	24.3	83	80
PuliFall (2022.10.25)	0	25	22.9	24.3	81	80
PuliFall (2022.10.26)	0	25	23.5	24.3	75	80

doi:10.6342/NTU202304440